scientific reports

Check for updates

OPEN

Comparing dormancy in two distantly related tunicates reveals morphological, molecular, and ecological convergences and repeated co-option

Laurel S. Hiebert[1,2,3], Marta Scelzo[1], Alexandre Alié[1], Anthony W. De Tomaso[2], Federico D. Brown[3,4 ✉] & Stefano Tiozzo[1 ✉]

Many asexually-propagating marine invertebrates can survive extreme environmental conditions by developing dormant structures, i.e., morphologically simplified bodies that retain the capacity to completely regenerate a functional adult when conditions return to normal. Here, we examine the environmental, morphological, and molecular characteristics of dormancy in two distantly related clonal tunicate species: *Polyandrocarpa zorritensis* and *Clavelina lepadiformis*. In both species, we report that the dormant structures are able to withstand harsher temperature and salinity conditions compared to the adults. The dormant structures are the dominant forms these species employ to survive adverse conditions when the zooids themselves cannot survive. While previous work shows *C. lepadiformis* dormant stage is present in winters in the Atlantic Ocean and summers in the Mediterranean, this study is the first to show a year-round presence of *P. zorritensis* dormant forms in NW Italy, even in the late winter when all zooids have disappeared. By finely controlling the entry and exit of dormancy in laboratory-reared individuals, we were able to select and characterize the morphology of dormant structures associated with their transcriptome dynamics. In both species, we identified putative stem and nutritive cells in structures that resemble the earliest stages of asexual propagation. By characterizing gene expression during dormancy and regeneration into the adult body plan (i.e., germination), we observed that genes which control dormancy and environmental sensing in other metazoans, notably HIF-α and insulin signaling genes, are also expressed in tunicate dormancy. Germination-related genes in these two species, such as the retinoic acid pathway, are also found in other unrelated clonal tunicates during asexual development. These results are suggestive of repeated co-option of conserved eco-physiological and regeneration programs for the origin of novel dormancy-germination processes across distantly related animal taxa.

To survive unfavorable environmental conditions, many animal species have evolved a remarkable strategy that allows them to reduce their metabolic rate and enter into a resting state; a process called dormancy[1–3]. Molecular and physiological mechanisms underlying dormancy across a variety of contexts in metazoans point to the existence of recurring processes[4–9]. For instance, the initial phases of dormancy involve the arrest of any ongoing development or cell proliferation and the onset of hypometabolism[10]. Stress response gene expression increases, enhancing stress tolerance and stabilizing cellular components. Metabolism shifts from carbohydrate to lipid combustion, and anabolism (such as DNA replication, transcription and translation) is radically attenuated[9,11]. During the maintenance phase of dormancy molecular chaperones, antioxidants, proteins responsible for DNA and chromatin stabilization or repair are produced, conferring environmental stress resistance[9,11].

[1]CNRS, Laboratoire de Biologie du Développement de Villefranche Sur-mer (LBDV), Sorbonne Université, Paris, France. [2]Molecular, Cellular and Developmental Biology, University of California, UCEN Rd., Santa Barbara, CA 93106, USA. [3]Departamento de Zoologia, Instituto Biociências, Universidade de São Paulo, São Paulo, SP, Brazil. [4]Centro de Biologia Marinha (CEBIMar), Universidade de São Paulo, São Sebastião, SP, Brazil. ✉email: fdbrown@usp.br; stefano.tiozzo@imev-mer.fr
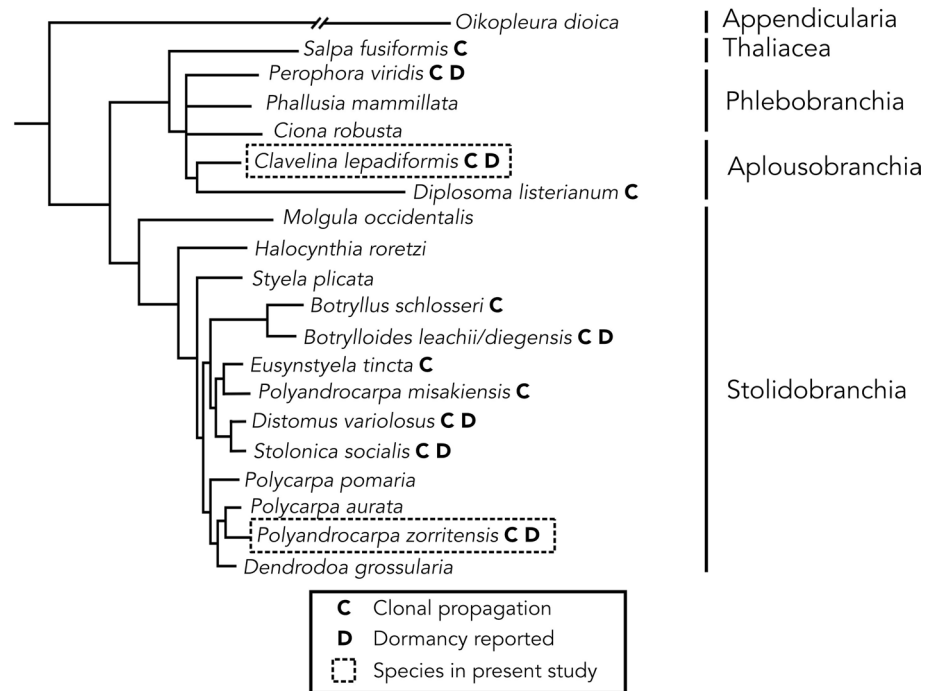
Figure 1. Consensus phylogeny of selected tunicate species indicating correlation between asexual cloning and dormancy. Orders are shown on the right. Species with clonal propagation are shown with "C" next to name. Species with capacity for dormancy are shown with a "D" next to name. The species in this study are boxed in a dashed line. Branch lengths and relationships are approximated from Alié et al.[82] (for Stolidobranchia), Delsuc et al.[34] (for Appendicularia, Thaliacea, Aplousobranchia, and Phlebobranchia except for *Perophora*), Tsagkogeorga et al. (2009) (for position of *Perophora*).

Among invertebrates, dormancy is found in 67 classes from 29 free-living phyla, and, depending on the species, can occur at different phases of their life cycle[2]. Many of the species that utilize dormancy are also clonal, meaning they grow via repeated rounds of asexual reproduction during which entire bodies are regenerated. In these clonal species, the dormant form has a morphologically simpler body plan that can survive in conditions that the feeding adults cannot. The dormant structures in clonal species include: podocysts in scyphozoan cnidarians[12], statoblasts in freshwater bryozoans[13], hibernaculae in kamptozoans[14,15], gemmules in sponges[1], and "survival buds", "resting buds", or "winter buds" (among other names) in tunicates[16,17].

In species that couple dormancy with asexual propagation, the dormant structures themselves are generally morphologically simple, but contain progenitor and nutrient storage cells that can initiate and support germination. For example, bryozoan statoblasts can survive desiccation, freezing, or even pass through the digestive tracts of aquatic vertebrates unharmed[3,18]. The statoblast consists of a germinal mass inside two sclerotized valves containing an outer layer of epithelial cells and an inner mass of yolk[19]. During germination, the epithelial cells undergo a thickening followed by invagination, and subsequent development follows that of typical bryozoan budding[20]. In some Demospongiae species, gemmules develop inside the sponge tissues. They are made up of a collagenous coat with siliceous spicules. Inside the coat are a few thousand pluripotent cells, each packed with nutrients in the form of yolk inclusions. During germination, cells inside migrate out of the coat, proliferate and differentiate to become juvenile sponges[21]. Only when the sponge dies do the gemmules have the capacity to germinate[21]. However, gemmules can remain dormant under certain low temperatures when separated from the rest of the sponge[21]. The stimulus responsible for germination appears to differ greatly across clonal dormancy-capable species, but typically germination occurs after separation from the adult under the proper environmental conditions.

To better understand the chain of events that span from the environmental triggering signals to the morphological and molecular changes that occur during the entrance and exit of a dormant state, we focused on the chordate subphylum Tunicata. In tunicates, dormancy has been reported exclusively in clonal species, i.e., species that undergo asexual reproduction by different types of budding[22] (Fig. 1). In clonal tunicates, budding is driven either by circulatory stem cells and/or by the ability of some epithelia to transdifferentiate[23–28]. While the mechanisms underlying budding differ across species and often involve non-homologous tissues and cells[22,23], their development generally converges at an early double-layered vesicle stage, reminiscent of a blastula, that eventually forms into a new feeding zooid[22,29]. In the colonial species for which a dormant stage has been documented, dormancy occurs by arresting the budding process[16,17,30–32]. While dormancy in some clonal tunicates is a mechanism of survival during adverse conditions (often called "hibernation" in harsh winters or "aestivation"
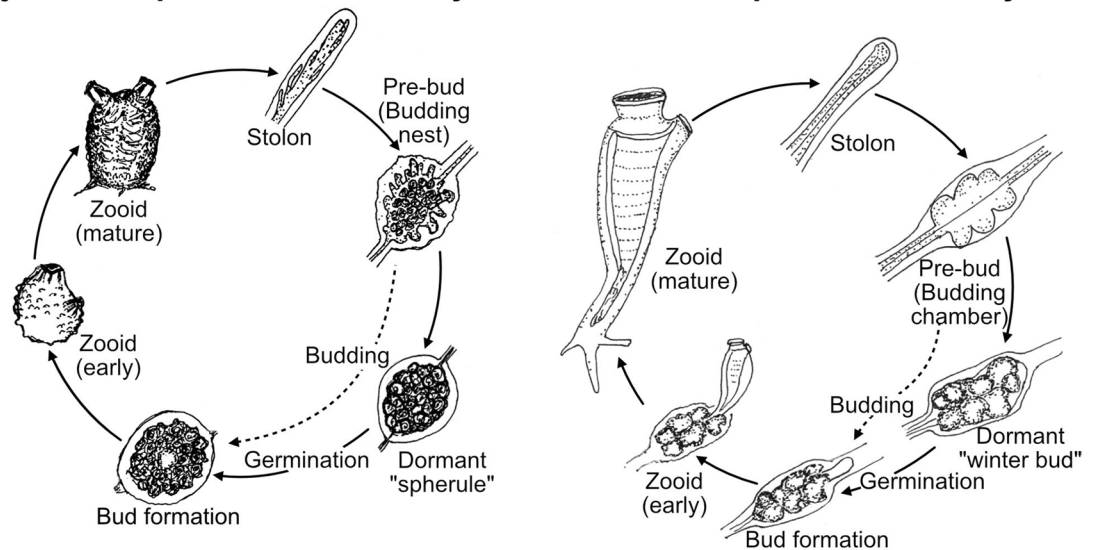
Polyandrocarpa zorritensis life cycle   *Clavelina lepadiformis* life cycle

Figure 2. Asexual life cycles of *Polyandrocarpa zorritensis* and *Clavelina lepadiformis*. At the base of mature zooids of both *P. zorritensis* and *C. lepadiformis*, extensions of the blood vessels encased in tunic, called stolons, protrude along the substrate. Along the stolons, ramifications of the internal blood vessels develop that we call "pre-buds" here (and are also known as "budding nests" in *P. zorritensis* and "budding chambers" in *C. lepadiformis*). The pre-buds swell and the surrounding tunic thickens to form structures called "spherules" for *P. zorritensis* or may accumulate opaque mass inside the vessel to become what has been called "winter buds" in *C. lepadiformis*. These dormant forms go on to germinate into a new zooid, but they have the capacity to withstand harsh conditions before germinating. Note that the pre-bud can also initiate the budding process without passing through a dormant state, as indicated by the dotted line in each life cycle.

in hot summers in other species), a period of zooid regression or loss of feeding is also proposed to have a role in rejuvenation[33].

In this study we chose two relatively distant species belonging to two tunicate orders: *Polyandrocarpa zorritensis* (Stolidobranchia) and *Clavelina lepadiformis* (Aplousobranchia) (Fig. 1[34]). We described behavior in laboratory conditions and analyzed their entrance and exit from the state of dormancy via anatomical and molecular characterizations. Dormant structures have been previously reported in the Atlantic and Mediterranean in *C. lepadiformis*[32,35–37]. In this study we document for the first-time seasonal variations of a *P. zorritensis* population in a temperate latitude and report the resistance of the dormant forms to variation in temperature and salinity in both species. We characterize and compare the morphological cellular structure and the transcriptomic profiles of dormant forms between these two species, and in order to better understand the molecular mechanisms involved in entry, maintenance, and release of dormancy, we present here the first results of a differential gene expression analysis of a number of stages of the life cycle of both species. Gene expression changes during dormancy in tunicates have not been previously studied.

Results

Life cycles of *Polyandrocarpa zorritensis* and *Clavelina lepadiformis*.
During *P. zorritensis* and *C. lepadiformis* asexual life-cycles (Figs. 2, 3, 4), epidermal projections of the zooids, called stolons, begin to ramify forming structures called "budding nests" (as in *P. zorritensis,* Fig. 3[38]) or to lobulated structures called "budding chambers" (as in *C. lepadiformis,* Fig. 4[35,39]), here for simplicity both referred as "pre-buds." Pre-buds can either give rise directly to buds and eventually develop into adult zooids in both species, or they can turn into dormant structures, i.e. orange spherical forms known as "spherules" in *P. zorritensis* (Figs. 2A, 3[38]) or white opaque dilations known as "winter buds" in *C. lepadiformis* (Figs. 2B, 4[35]).

P. zorritensis spherule and zooid turnover conforms with seasonal changes.
To evaluate the presence of dormant versus actively growing stages in their natural habitat, a population of *P. zorritensis* located in La Spezia (Italy) was monitored over 2 years (from August 2017 to May 2019) with two to three observations per season (Fig. 5). In summer, fall, and winter the colonies formed dense clusters of zooids, and dormant spherules were connected to the colony by stolons on the bottom sides of these clusters (Fig. 5B). During two springs (March 2018 and May 2019) no zooids were observed and the colony consisted solely of isolated spherules (as in Figs. 3E, 5C), attached to the boat mooring lines, and covered by epibionts. Spherules collected over the year (2018–2019) showed differences in average diameter (Fig. 5E). The average spherule size was significantly larger during fall than in winter, and significantly larger in fall than spring (RM-ANOVA, $p < 0.03$; Fig. 5E).

Combining our observations with the monthly temperature ranges of seawater in La Spezia from NOAA Sea Surface Temperature satellite data (AVHRR Pathfinder SST[40]) the largest spherules were obtained in the
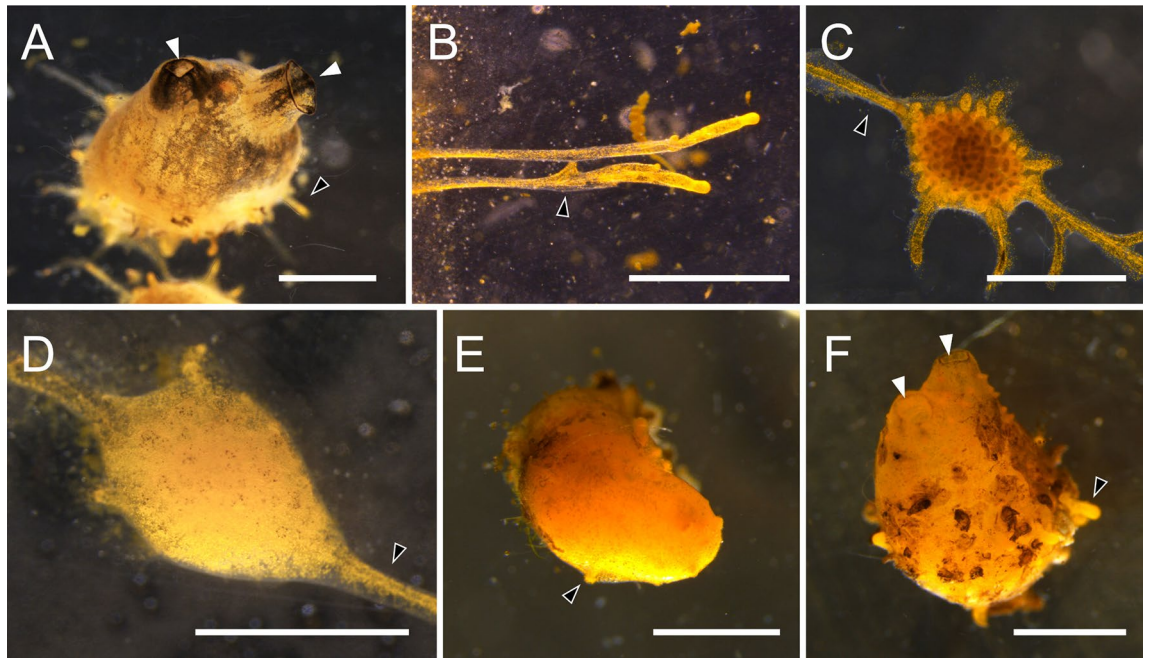
Figure 3. Photomicrographs of *Polyandrocarpa zorritensis* asexual stages. (**A**) Zooid. Siphons (white arrowheads) open for feeding. Stolons (black arrowhead marks one as an example) help attach the zooid to the substrate, and have begun to grow laterally. (**B**) Stolons attached firmly on a glass slide. Lower stolon starting to ramify (black arrowhead) where new pre-bud will likely develop. (**C**) Pre-bud still attached to "parental" zooid by stolon (black arrowhead), thus no bud tissues have begun to develop. Ramifications of vasculature seen within the structure through the tunic. (**D**) Early spherule, as indicated by thickened tunic, which obscures the vascular ramifications inside. This spherule remains attached to the zooid by the stolon, and thus budding has not yet initiated. (**E**) Detached spherule undergoes germination, as stolonal outgrowths form (black arrowhead). (**F**) Young zooid that arose from a hatched spherule. Siphons are open (white arrowheads), suggesting that filter feeding has been initiated. Stolon (black arrowhead) begins to grow outward. Scale bars are all 1 mm.

fall and early winter before the zooidal degeneration event that occurred at the end of the winter (Fig. 5D, E). During the zooid-free period in the spring, the spherules became smaller, presumably using up their nutrient reserves (Fig. 5D, E).

Entry into and exit from dormancy in *P. zorritensis* and *C. lepadiformis*. To test some possible abiotic environmental parameters influencing entry and exit of dormancy, small colonies of field-collected *P. zorritensis* (comprising zooids, budding nests, developing buds, and stolons) were maintained in controlled conditions in a flow-through aquarium system at 24 °C and fed with a diet of living and concentrated algae. In order to determine if temperature would induce the production of dormant spherules, we removed a few small colonies (number of zooids = 17; number of stolons = 24; number of developing nests = 5; number of non-abscissed nests = 5) from the aquarium system and placed them at lower temperatures (10 °C). Over the course of 2 months, we observed the production of dormant spherules. The zooids, when still alive, showed closed siphons and a low response to mechanical stimulation (n = 15). The buds that we experimentally detached (abscised) from their "parent" zooid, which had already started the budding process, arrested development and degenerated (n = 5). Stolonal growth continued, allowing the growth of the present budding nests (n = 5) and the development of new ones (n = 5). These structures were externally similar to spherules; they were dome-shaped and the tunic was so thick that it obscured internal vascular ampullae. Histological and ultrastructural observations were performed, showing that these structures were the same as spherules collected from the field[38]. This represented the first successful production of dormant-stage specimen of this species in laboratory conditions.

To identify the colony tissue sensitivity and the precise temperature that triggered dormancy in *P. zorritensis*, we exposed the following groups (1) spherules collected in the field (n = 10) stored at 10 °C, (2) zooids with spherules (n = 3) produced in laboratory after transfer at 10 °C, and (3) budding nests (n = 3) produced in the laboratory after germination of spherules and stored at 24 °C to four different temperatures (8 °C, 12 °C, 17 °C, 22 °C) and documented their development for 6 weeks. At the lowest temperature (8 °C) all the zooids died while the spherules and the budding nests did not germinate. At 12 °C, half of the zooids died or detached from the glass slide; stolonal growth was arrested; and new budding nests or developing buds did not form after 6 weeks. At this temperature all the spherules (collected in the field and produced in the laboratory) were activated and produced new zooids in 30–35 days. At 17 °C the zooids stayed alive and well-attached to the glass slide, all spherules germinated (after about 20 days) and new stolons, budding nests, and spherules were produced. At 22 °C the spherules and budding nests were rapidly activated (after 2 weeks new zooids were visible). However, half of the zooids died or were detached and few new stolons and nests were produced. These results suggested
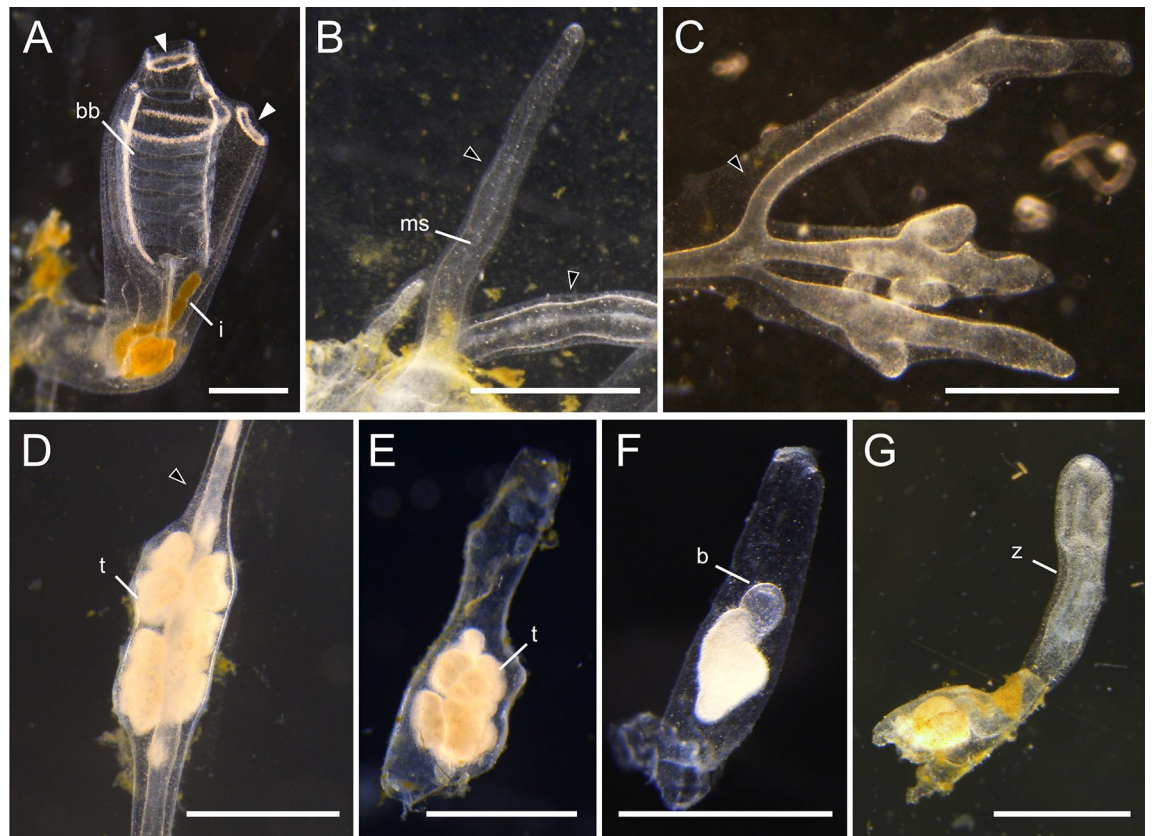
Figure 4. Photomicrographs of *Clavelina lepadiformis* asexual stages. (**A**) View of a feeding zooid with siphons (white arrowheads), branchial basket ("bb"), and intestine ("i"). (**B**) Stolons (marked with black arrowheads) protruding from zooid allow for attachment to substrate and for production of pre-buds. Mesenchymal septum ("ms") indicated within stolon. (**C**) Stolons (marked with black arrowheads) undergo branching morphogenesis near the tips and begin to form the pre-buds (also called budding chambers in this species). (**D**) Early winter bud in a stolon still attached to the zooid. It has accumulated mass of trophocytes ("t") inside as indicated by opaque white material. Stolon marked with white arrowhead. (**E**) Detached winter bud with a large mass of trophocytes ("t"). (**F**) Winter bud undergoing early steps of germination. The germinating bud (b) seen as a small transparent bump above the trophocyte mass. (**G**) Late germination stage showing young zooid ("z") that arose from winter bud. Siphons are not yet visible. Remnants of winter bud remain and continue to supply nutrition to zooid until it begins to feed on its own or until it runs out of the supplied nutritive material. Scale bars are all 1 mm.

that the budding nests transferred to 8 °C, 12 °C, 17 °C could form spherules. When the spherules (collected in the field or produced in the laboratory, both stored at 10 °C) were transferred to lower temperatures (from 10 to 8 °C) they did not activate; however, when they were transferred to slightly higher temperatures (from 10 to 12 °C) germination was activated and new zooids were generated. We noted that spherule germination was days faster at higher temperatures, but was not synchronized across specimens.

The ability to produce dormant forms under laboratory conditions was tested also in *C. lepadiformis*. Specimens of *C. lepadiformis* were collected at the same site as *P. zorritensis* and were cultured on glass slides at 18 °C. As previously described by other authors[32,35,37] the zooids emitted vascular stolons as prolongations of the postabdomen (Fig. 4B). The stolonal tip sometimes started to bulge forming one or more lobes, which looked more pale and whitish than the rest of the stolon (Fig. 4C). These structures represent the budding chambers, in which the budding process takes place once the hemocyte circulation is interrupted between the zooid and the budding chamber. At this temperature, other structures similar to budding chambers but more compact and whitish are produced along the stolon; they represent the winter buds, which are able to resist cold temperature according to other authors (Fig. 4D[39,41]). Our results showed that the production of *C. lepadiformis* dormant forms, the winter buds, occurred at 18 °C in laboratory conditions; and that similarly to budding chambers, the winter buds could be activated by isolation from the stolon. According to the above-mentioned authors, the milky coloration of winter buds is due to accumulation of trophocytes, i.e., hemocytes specialized for storage and transport of nutrients.

Viability and range of resistance of *P. zorritensis* spherules and *C. lepadiformis* winter buds. In order to determine the ability of dormant forms to resist sudden environmental changes, we exposed spherules and adult zooids of *P. zorritensis* to abrupt shifts in temperature (− 20 °C to 37 °C) and salinity (10–44 ppt) for
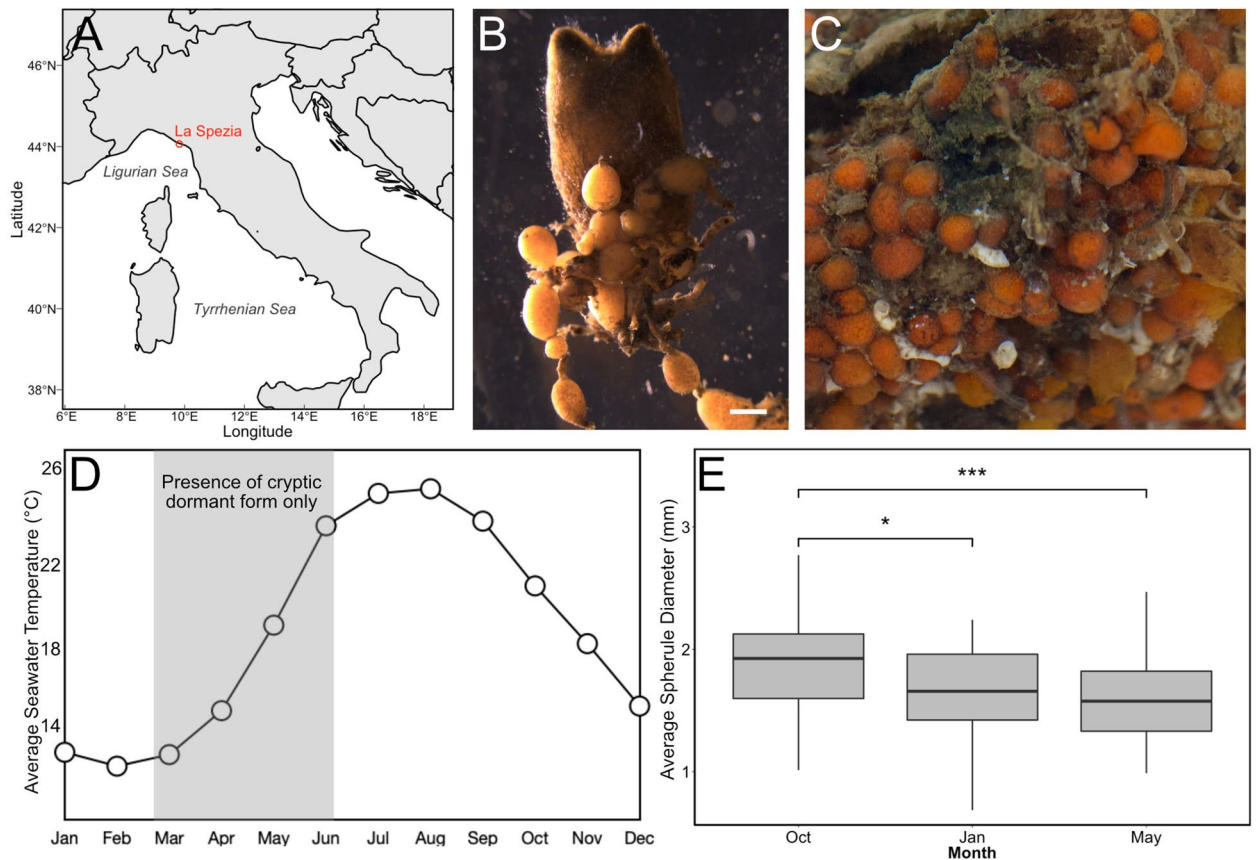
Figure 5. Field colony dynamics of *Polyandrocarpa zorritensis* in La Spezia, Italy. (**A**) Map shows collecting location in La Spezia in the NW of Italy. (**B**) Zooid collected from the harbor of La Spezia, with spherules attached along stolonal projections. Scale bar is 2 mm. (**C**) Close-up of dormant spherules. (**D**) Average surface seawater temperature in La Spezia (NOAA Sea Surface Temperature satellite data from AVHRR Pathfinder SST). Shaded area indicates the period that animals exist in the cryptic dormant form. The rest of the year, both zooids and spherules are found on the ropes in the harbor. (**E**) Graph showing the change in average spherule size (n = 45) over the year, with the largest spherules found in October, and the smallest spherules in May.

24 h. Following the stress treatment, the specimens were transferred to 24 °C and the viability of zooids and the germination of dormant forms were observed after 2 weeks. *P. zorritensis* zooids survived a minimal range of conditions (between 18 and 28 °C and between 30 and 38 ppt), while spherules resisted a wider range of conditions (temperature fluctuation between 0 and 32 °C and salinity between 15 and 45 ppt) (Fig. 6).

We repeated the same experiment with winter buds and *C. lepadiformis* zooids. Both stages were exposed for 24 h to a wide range of temperatures (− 20 to 37 °C) and water salinity (10–44 ppt). Then, the specimens were transferred to 24 °C and the viability of zooids and the germination of dormant forms were observed after one week. *C. lepadiformis* zooids were more resistant to lower temperatures (between 0 and 28 °C) and higher salinity (30–45 ppt) than *P. zorritensis*. Winter buds resisted a wider range of conditions compared to zooids (temperatures between 0 and 32 °C and salinity between 15 and 45 ppt), similar to *P. zorritensis* spherules (Fig. 6).

Morphology of *P. zorritensis* spherules and *C. lepadiformis* winter buds. From a histological perspective, a spherule appears as a cluster of monolayered chambers, the ampullae, interconnected by vessels, all embedded in a thick extracellular matrix called tunic (Figs. 7E, 8A[38]). Tunic fibers of spherules are thicker than in the budding nests (∼ 20 μm vs ∼ 5 μm[38]). The epithelium of the ampullae is formed by cylindrical columnar cells of ∼ 10 μm in length and ∼ 5 μm in width (Fig. 7F). The cytoplasm of the epithelial cells is filled with two types of electron-dense inclusions: small electron-dense granules of glycogen (0.5–1 μm) and uniform electron-dense granules of lipids (2–5 μm) (Fig. 7G). The ampullae and vessels are filled with a heterogeneous population of hemocytes, among which it is possible to identify round undifferentiated cells of 5 μm diameter (Fig. 7H) which have a large nucleus-to-cytoplasm ratio, a prominent nucleolus, and with poorly developed endoplasmic reticulum and scarce mitochondria, reminiscent of ascidian circulatory stem cells referred to as hemoblasts[25,42].

In a *C. lepadiformis* winter bud, the epidermal cells around the vascular lumen are filled with electron-dense lipid inclusions in the cytoplasm—similarly to *P. zorritensis* spherules, which include small glycogen granules, homogeneous electron dense granules, and heterogeneous electron dense inclusions. The vascular lumen of the winter bud contains many more mesenchymal cells and more densely-packed cells than the stolonal lumen. The winter bud lumen contains large cells of more than 20 μm that appear to be macrophages (Fig. 7C). The
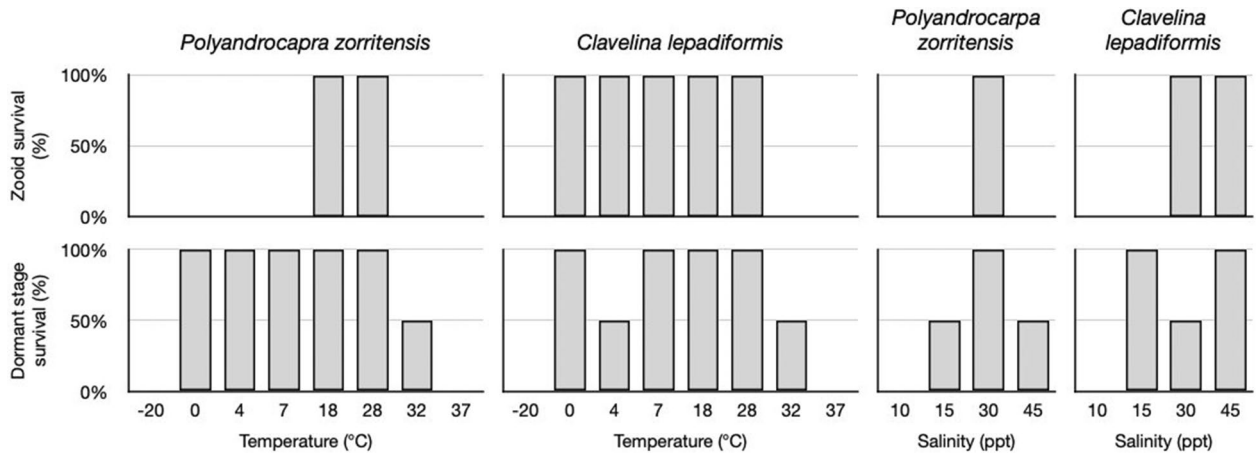
Figure 6. Dormant stages have broader capacity for survival, compared to zooids, in response to environmental stressors. Graphs of percent survival after 48 h exposure to the indicated temperatures and salinity (n = 2 per treatment) for *P. zorritensis* and *C. lepadiformis*.Top row shows survival rates of zooids. Bottom row shows survival rates for dormant structures (spherules for *Polyandrocarpa zooirtensis* and winter buds for *Clavelina lepadiformis*).
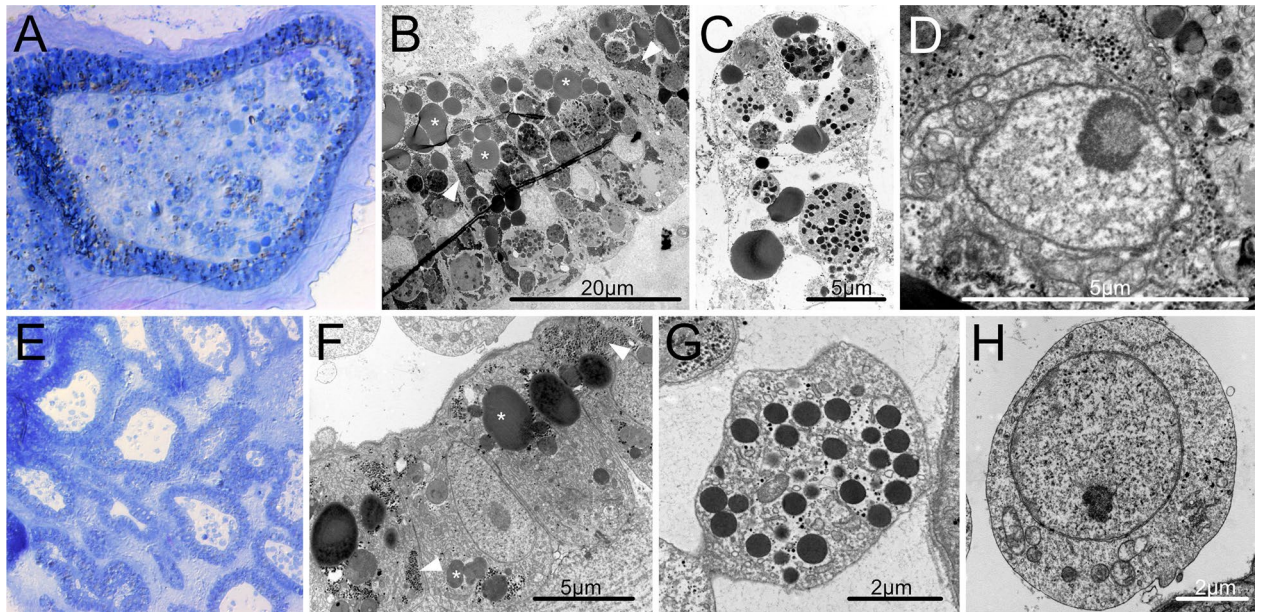

Figure 7. Cell types in dormant stages of *Clavelina lepadiformis* and *Polyandrocarpa zorritensis* include nutrient storage cells and putative stem cells. (**A–D**) *C. lepadiformis*: (**A**) Methylene blue staining of winter bud histological section shows a thick layer of epithelial cells surrounded by tunic and enclosing abundant mesenchymal cells. (**B**) TEM image of epithelial cells, many with lipid and glycogen inclusions, labeled with asterisk and white arrowheads, respectively. (**C**) TEM image of a phagocyte with contents inside mesenchymal space. (**D**) Putative hemoblast cell inside mesenchymal space, as indicated by large nucleolus and small cell size (about 5 microns). (**E–H**) *P. zorritensis*. (**E**) Methylene blue staining of spherule histological section shows numerous ampullary spaces lined with epithelium and filled with sparse hemocytes. (**F**) TEM close-up image of epithelial cells of ampulla, showing inclusions of lipids (asterisks) and glycogen (white arrowheads). (**G**) Example of a mesenchymal cell with inclusions. (**H**) TEM image of putative hemoblast cell within the mesenchymal space, as indicated by large nucleolus, small cell size, and round cell shape.

phagosomes of the macrophage-like cells are filled with material containing electron-dense inclusions (Fig. 7C). These cells are tightly packed and surrounded by non-cellular debris (Fig. 7A–D).

In order to test if developmental events in spherule germination resemble budding in *P. zorritensis* budding nests, spherules maintained at 10 °C were transferred to a higher temperature (24 °C) and fixed after 48 h. In developing spherules, the vascular epidermis invaginated in a similar way as in developing budding nests (Fig. 8B). These results suggest that the epidermal morphogenetic movements that occurred in germinating
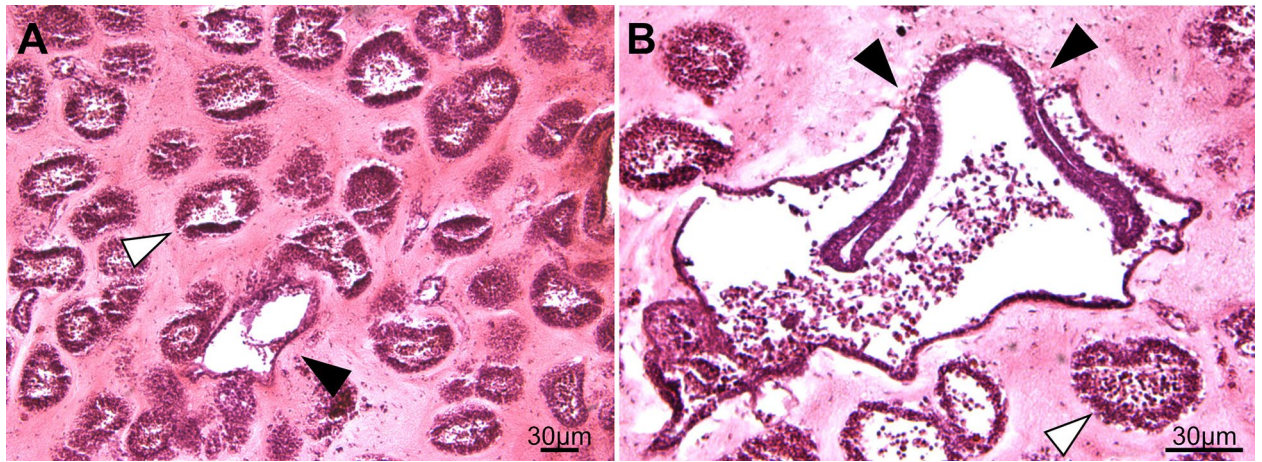
Figure 8. Germination transition in *P. zorritensis*. Transversal histological sections stained with hematoxylin and eosin of germinating spherule after 48 h at 24 °C. (**A**) The central vessel (black arrowhead) is distinguishable from the ampullary ramifications (one example marked with white arrowhead). (**B**) In a section through the center of the spherule, the vascular epidermis is invaginating (black arrowheads indicate location of the invaginations). White arrowhead indicates ampullary ramification.

spherules resemble the vasal budding processes previously described in the development of *P. zorritensis* budding nests[38].

Transcriptomic signatures of *P. zorritensis* spherules and *C. lepadiformis* winter buds show genes involved in the maintenance of dormancy. In order to elucidate the molecular signature of dormancy, we examined gene expression across life stages in both *P. zorritensis* and *C. lepadiformis* (Fig. 9). We conducted RNAseq and compared expression in five tissue types: zooids, pre-buds, stolons, dormant stages, and germinating tissues. PCA analyses showed correlation between the replicates, and separation between tissue types (Fig. 9). Of the orthologous DEGs that were up-regulated in dormant tissues in both species, 530 genes were shared. Among the shared up-regulated genes in dormancy, we examined KEGG pathway enrichment and found an over-representation of genes in a number of pathways, such as the HIF-α pathway and the insulin signaling pathway (Fig. 10; Supplementary Figure S1).

We also examined upregulated transcription factors in dormancy that were either shared between species or found exclusively in one species (Fig. 10C). Some of the shared upregulated transcription factors were involved in HIF-α signaling, such as a hypoxia inducible factor alpha (HIF-α), and in insulin signaling. Additionally, we found shared up-regulation of a number of genes implicated in the modulation of stem cell maintenance, proliferation, and differentiation. These included: orthologues of AP-1 transcription factor (fos and jun), NK4 homeobox, nuclear receptor subfamily 4 group A (NR4A1-3), retinoic acid receptor beta (RAR-A/B/G), and signal transducer and activator of transcription (STAT5-7). Some of the shared transcription factors upregulated in dormancy have gene silencing or chromatin remodeling functions, such as methyl-CpG binding domain protein 2 (MBD2-4) and male-specific lethal 3 (MSL3)[43,44]. Orthology was confirmed using phylogenetic analysis (Supp. Figure S3).

Exit from dormancy shares morphological/molecular features as in whole body regeneration or budding in colonial ascidians. We found that 674 genes are up-regulated during germination in both species (Fig. 11A). KEGG pathways upregulated in this shared set of genes include many metabolic pathways (Fig. 11B). We also found a number of shared up-regulated transcription factors. This includes developmental genes such as NK4, grainhead-like transcription factor (GRHL1/2/3), and a distal-less homeobox (DLX1/6), and retinoic acid receptor beta (RAR-A/B/G) (Fig. 11C). Interestingly, some transcription factors that showed upregulation in germination are also genes that we found to be upregulated in dormancy, including NK4, RAR-A/B/G, and forkhead box H (FOXH). Orthology was confirmed using phylogenetic analysis (Supp. Figure S3).

Discussion
Ecological consequences of dormancy in clonal species. We report the disappearance of zooids of *Polyandrocarpa zorritensis* at the end of the winter in NW Italy, with the maintenance of only a cryptic dormant form: small spherules hidden under epibionts. Such small, relatively undifferentiated, and practically unrecognizable structures remain dormant for months and have the ability to reconstitute a thriving population of differentiated feeding animals when conditions improve. By the end of the spring, through a mass-scale regeneration event, spherules are able to restore the entire population of filter-feeding colonies. Our data on spherule diameter over the year suggests that spherules get smaller as the zooid die-off period approaches, which may be due to the nutritive and energetic demands of cells within the spherules over the year. Winter buds of *Clavelina lepadiformis* have also been found to exist in the absence of zooids. Winter buds without zooids have been documented in the North Sea in the winter months[36,45] in the summer months in the eastern Mediterranean, and both *C. lepadi-*
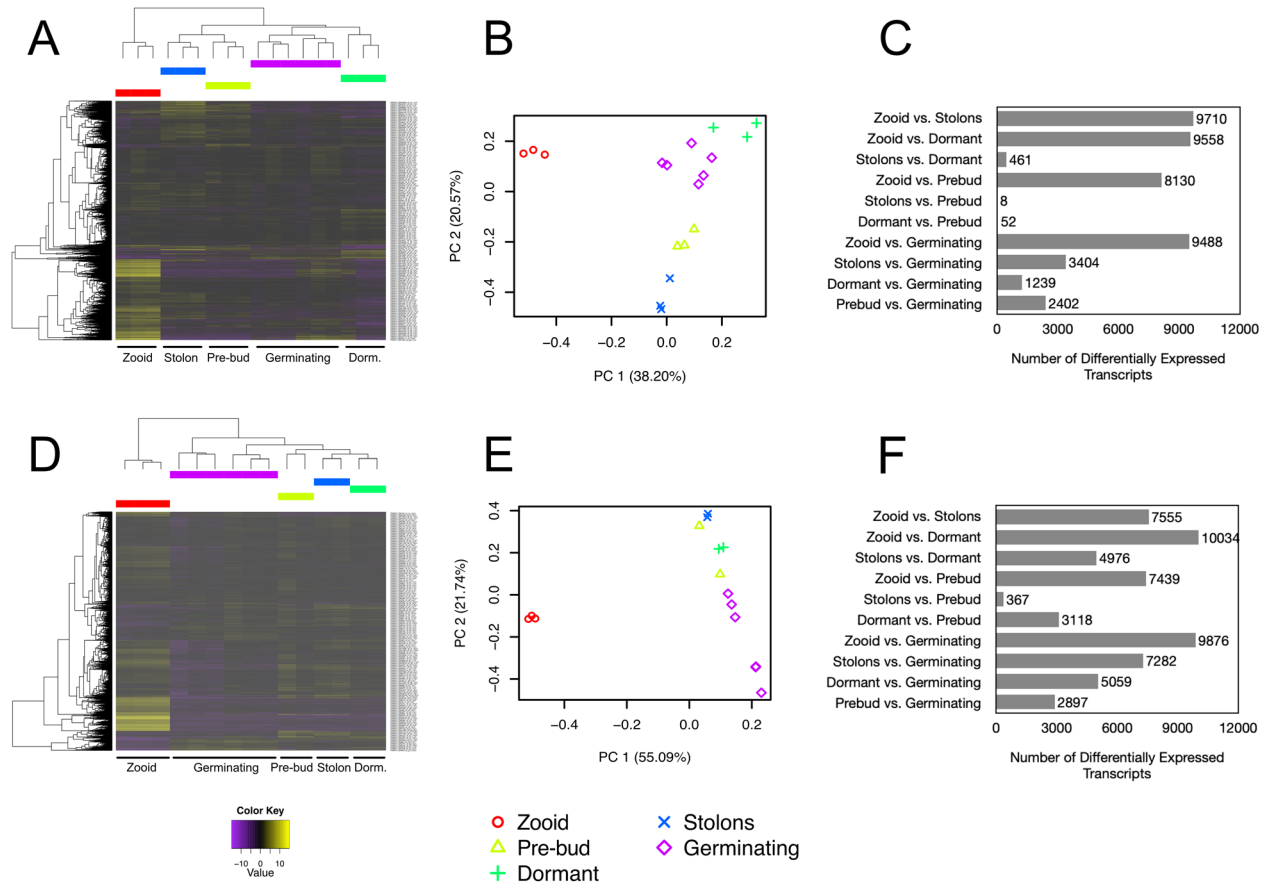
Figure 9. Differentially expressed transcripts during life stages in *Polyandrocarpa zorritensis* and *Clavelina lepadiformis*. Heatmaps of differentially expressed transcripts across samples: (**A**) *P. zorritensis* and (**D**) *C. lepadiformis*; each row represents expression value of a single transcript as shown in the color key below plots, violet indicates low expression and yellow indicates high expression; columns show clustered life stage replicates, bars in red = zooid, blue = stolon, yellow = pre-bud, green = dormant, and magenta = germinating stage. Principal Component Analysis showing relationships among and across samples: (**B**) *P. zorritensis* and (**E**) *C. lepadiformis*. Key below indicates colored symbols for each life stage sample type. Number of differentially expressed transcripts in each pairwise comparison between sample types for each species: (**C**) *P. zorritensis* and (**F**) *C. lepadiformis*.

Figure 10. Shared up-regulated transcripts and pathways during dormancy in *P. zorritensis* and *C. lepadiformis*. (**A**) Venn diagram showing the number of orthologous upregulated transcripts during dormancy in *P. zorritensis* and *C. lepadiformis*. (**B**) KEGG pathway terms enriched in the overlapping set of 530 transcripts upregulated in both species. (**C**) Transcription factors upregulated in dormancy in both species.

A

Polyandrocarpa zorritensis   *Clavelina lepadiformis*

2222   674   718

Differentially expressed in germination

B

GO Analysis

Ribosome
Glycosphingolipid biosyn. lacto and neolacto
Staphylococcus aureus infection
Cell adhesion molecules (CAMs)
Synthesis and degradation of ketone bodies
Galactose metabolism
Glycosaminoglycan biosynth. keratan sulfate
Spliceosome
Herpes simplex infection
Complement and coagulation cascades
Alanine, aspartate and glutamate metabolism
Insulin resistance
mRNA surveillance pathway
Mineral absorption
Insulin signaling pathway
Fanconi anemia pathway
Legionellosis
Butanoate metabolism
Central carbon metabolism in cancer

Enrichment score

−log10(PValue): 20, 15, 10, 5

Number of genes: 10, 20, 30, 40

C

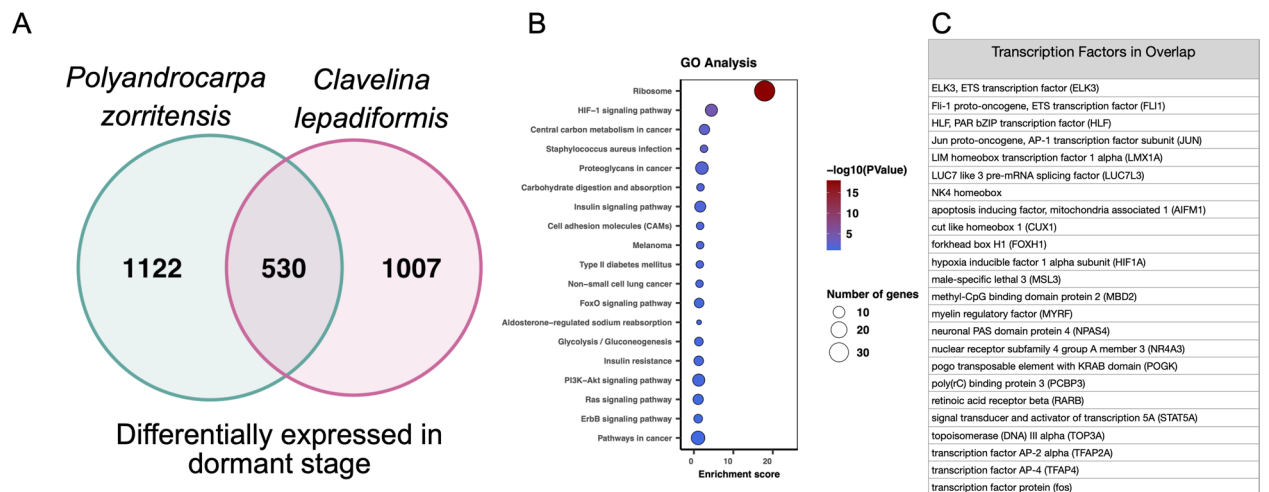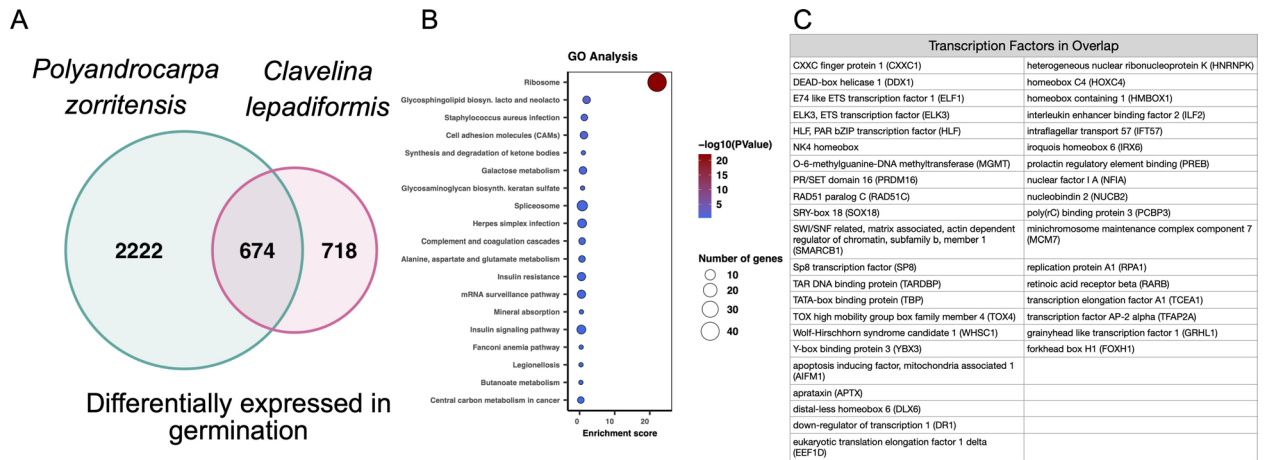| Transcription Factors in Overlap	
CXXC finger protein 1 (CXXC1)	heterogeneous nuclear ribonucleoprotein K (HNRNPK)
DEAD-box helicase 1 (DDX1)	homeobox C4 (HOXC4)
E74 like ETS transcription factor 1 (ELF1)	homeobox containing 1 (HMBOX1)
ELK3, ETS transcription factor (ELK3)	interleukin enhancer binding factor 2 (ILF2)
HLF, PAR bZIP transcription factor (HLF)	intraflagellar transport 57 (IFT57)
NK4 homeobox	iroquois homeobox 6 (IRX6)
O-6-methylguanine-DNA methyltransferase (MGMT)	prolactin regulatory element binding (PREB)
PR/SET domain 16 (PRDM16)	nuclear factor I A (NFIA)
RAD51 paralog C (RAD51C)	nucleobindin 2 (NUCB2)
SRY-box 18 (SOX18)	poly(rC) binding protein 3 (PCBP3)
SWI/SNF related, matrix associated, actin dependent regulator of chromatin, subfamily b, member 1 (SMARCB1)	minichromosome maintenance complex component 7 (MCM7)
Sp8 transcription factor (SP8)	replication protein A1 (RPA1)
TAR DNA binding protein (TARDBP)	retinoic acid receptor beta (RARB)
TATA-box binding protein (TBP)	transcription elongation factor A1 (TCEA1)
TOX high mobility group box family member 4 (TOX4)	transcription factor AP-2 alpha (TFAP2A)
Wolf-Hirschhorn syndrome candidate 1 (WHSC1)	grainyhead like transcription factor 1 (GRHL1)
Y-box binding protein 3 (YBX3)	forkhead box H1 (FOXH1)
apoptosis inducing factor, mitochondria associated 1 (AIFM1)	
aprataxin (APTX)	
distal-less homeobox 6 (DLX6)	
down-regulator of transcription 1 (DR1)	
eukaryotic translation elongation factor 1 delta (EEF1D)	

Figure 11. Shared up-regulated transcripts and pathways during germination in *P. zorritensis* and *C. lepadiformis*. (**A**) Venn diagram showing the number of orthologous upregulated transcripts during germination in *P. zorritensis* and *C. lepadiformis*. (**B**) KEGG pathway terms enriched in the overlapping set of 674 transcripts upregulated in both species. (**C**) Transcription factors upregulated in germination in both species.

formis and *C. gemmae* regress during summer months (called aestivation) in the western Mediterranean[46–48]. These results show that the dormant stages of both *C. lepadiformis* and *P. zorritensis* are resistant to extremes in temperature and salinity. Thus, this linked capacity for dormancy and regeneration is likely an important adaptation that allows these species to survive drastic seasonal changes.

Our field observations on *P. zorritensis* suggest that even in conditions favorable for budding, the dormant forms are continuously produced as stolon mats under the colony and are ready to assure survival if conditions become adverse. The pre-buds and dormant structures are produced throughout the time that the filter-feeding zooids are also present. As soon as these structures detach from the parent zooid, budding is triggered. However, if the stolonal connection is maintained, the pre-buds continue to grow in size, acquiring additional nutrients, and budding is inhibited. This occurs once the zooids have propagated to take up significant space such as to limit available surface area for further zooid production. When the zooids are highly packed together, the pre-buds are protected from abscission, and when they maintain the connection with the parent, they continue to grow into larger dormant structures. The connection with the parent is also maintained more readily at low temperatures in laboratory conditions.

The capacity for dormancy followed by regenerative germination allows for survival over time periods of unfavorable conditions, but this adaptation likely allows for survival across space and into new habitats. Both *P. zorritensis* and *C. lepadiformis* are well-documented invasive species in numerous regions of the world. *C. lepadiformis,* which is a native of the Mediterranean Sea, Atlantic subarctic regions (i.e., Norwegian Sea and Greenland), and Bay of Biscay, has successfully spread to the coastline of South African, the coasts of North and Central America, and Brazil[49–52]. *P. zorritensis*, described for the first time in Peru[53], has been reported in the last decades at sites all over the world, especially in harbors[54,55]. In the Mediterranean Sea, *P. zorritensis* has been recorded in Italy[56–59], Spain[60] and very recently in France, in the Thau pond (reported on the DORIS website https://doris.ffessm.fr/Especes/Polyandrocarpa-zorritensis-Polyandrocarpe-de-Zorritos-5004). Tolerance to a range of environmental conditions has been proposed to help account for its invasive success. The physiological responses to abiotic parameters such as light, pressure, and salinity have been investigated in the larvae of *P. zorritensis*[61–63], but these results were insufficient to explain the rapid expansion of this species. Our data show that *P. zorritensis* spherules are capable of resisting a wide range of environmental extremes, and these small structures can be easily transported and reestablish a new colony. Thus, *P. zorritensis* invasions in semi-enclosed basins with peculiar abiotic conditions, like the case of Taranto Sea in southern Italy[58], may have been facilitated by the resistance of the spherules to large changes in salinity and temperature. Overall, the unique dormant phase of the life cycle and the ability to survive in a non-feeding state may underline the extreme success in invasion ability of these species.

Convergences in cellular makeup of dormant structures. The dormant structures in both *C. lepadiformis* and *P. zorritensis* contain a relatively small amount of cell morphotypes. Those include cells that store the nutrients for the maintenance of the dormant stage, cells that have the potential to contribute to the development of new buds (undifferentiated mesenchymal cells), and cells with protective function, including tunic-secreting cells. In many dormant tunicates, specialized mesenchymal cells called trophocytes, storage cells, or granular amebocytes, accumulate nutritive reserves that are used during the development of the new zooid[17,30,64–66]. In *C. lepadiformis*, the trophocytes accumulate reserves by sequestering breakdown products of dying and degenerating zooids[67–69]. While a few authors speculated that these cells represent the undifferentiated regenerative cells[36,70], most agree that they correspond to large phagocytic migratory cells that contain cytoplasmic glycoproteins and other inclusions, but have no direct role during the differentiation occurring during germination[71–73]. Fisher[73] also documented "cell excretions", which may be decaying cell material that is excreted into the vasculature to be used for nutrition of the developing bud. Fujimoto and Wanatabe[65] examined budding tissues in

Polyzoa vesiculiphora and found the occurrence of granular amebocytes that contained glycogen particles, lipid droplets, large protein granules, and autophagosomes, which they classified as trophocytes. They documented that these cells were phagocytized over the course of bud development, then disappeared, suggesting that they are important for nutrient supply to the bud. In our ultrastructural analysis of *C. lepadiformis* winter buds, we documented large cells filled with phagosomes and inclusions of glycogen and lipids, which we also believe represent the trophocytes. We also found lipid and glycogen-rich cells present in the epithelia of the winter bud in *C. lepadiformis*. In contrast, we did not find any mesenchymal trophocytes in *P. zorritensis* that could be used for nutrition, and therefore we propose here an alternative strategy this species may use to sequester nutrients within the dormant form. The vascular epithelium of *P. zorritensis,* unlike *C. lepadiformis,* is highly ramified within the spherule, providing many epithelial cells, filled with nutrient inclusions of lipids and glycogen, that may be used during dormancy and to support germination. Thus, the two species have acquired unique adaptations for endowing the dormant form with distinct supplies of nutrition to last through the dormant period and during germination.

The pluripotent cells or tissues that give rise to the mesodermal layer (the mesentoblast or "inner vesicle" of the characteristic double-vesicle stage of bud development) differs across diverse tunicate species. Early work showed that the inner vesicle in *C. lepadiformis* arises from cells from the stolonal septum[35,64,71,74–76] whereas Fisher[73] cultured winter bud cells and found that the small undifferentiated cells contributed to the formation of new budding tissue. Our ultrastructural examination of winter buds led to the identification of small cells with a prominent nucleolus, which likely represent the undifferentiated cells that give rise to the new buds. However, we could not clearly visualize the stolonal septum within the winter bud. So, how the septum and undifferentiated cells play a part in the budding process in both normal buds and winter buds is still unclear. *P. zorritensis*, on the other hand, lacks a stolonal septum, and the source of the inner vesicle in budding nests is known to be the vascular epithelium[38]. However, we did observe mesenchymal putative stem cells (hemoblasts) in the vasculature of *P. zorritensis* during dormancy. A role for hemoblast cells during germination is possible, but has not been documented.

Shared molecular mechanisms of dormancy across distantly related tunicates.
Our analysis involves two phylogenetically distant tunicate species that most likely have independently acquired dormancy. Both species express a number of common genes and pathways during the dormant phase. For example, both species show up-regulation of key components of the HIF1-α signaling pathway and the insulin signaling pathway. HIF-α signaling is utilized in other species during dormancy[9]. HIF-α signaling induces a metabolic rewiring that promotes anaerobic glycolysis and a shift from glucose to fatty acid combustion that helps maintain cellular quiescence[9]. Further, the insulin signaling pathway has been shown to be key to the control of diapause in some insects[6], as well as the dauer diapause stage in nematodes[77,78]. In low nutrient situations, insulin signaling is reduced, which activates FoxO/DAF-16, which lowers the production of ROS to protect against oxidative damage, and regulates both the formation and morphogenesis of the diapause stage[9,78]. These mechanisms have also been described during mammalian hibernation and cellular quiescence in hematopoietic stem cells[9]. Our findings further support the occurrence of a core program of dormancy in animals that is related to the physiological and developmental demands of this unique stage.

Among the upregulated genes during dormancy in both *P. zorritensis* and *C. lepadiformis* we found transcription factor AP-1 (activating protein-1), which is known to regulate gene expression in response to various stimuli, such as stress, hypoxia, or growth factors[79]. The AP-1 family of transcription factors contains homodimers and heterodimers of fos and jun subunits, among others[80]. We find *fos* and *jun* up-regulation in dormancy in the two tunicate species we examined. AP-1 is known to have a role in regulation of cellular proliferation, senescence, and differentiation, including in the context of regeneration, where these genes are often some of the first responders after injury[80,81]. Thus, AP-1 may play an important role in maintaining cells in a non-proliferative state or undifferentiated state during dormancy. Sensing changes in environmental conditions is key for sessile organisms to make decisions about resources committed to growth and development. As oxygen levels and nutrient availability are two of the most variable environmental parameters, it is not surprising that both HIF, insulin signaling pathways, as well as quick-responding genes such as AP-1 family factors would be shared regulators of dormancy. In the future, higher resolution lab studies with precisely manipulated food and oxygen levels could be used to compare responses between species, and identify the order of molecular events.

Regenerative emergence (germination).
In both *P. zorritensis* and *C. lepadiformis*, the dormant state appears to be overlayed onto the pre-budding stage of the life cycle. As dormancy ends, and germination begins, the budding process resumes. We found a number of transcription factors that are highly expressed in this germination stage that are shared between both species. For instance, NK4 (the tunicate homologue of vertebrate Nkx 2.3/5/6) was previously found expressed at the onset of two independently evolved types of budding, vasal budding in *P. zorritensis* and peribranchial budding in *Botryllus schlosseri*[82]. NK4 is also expressed in various embryonic and larval territories and notably required for heart formation[83,84]. The high expression of NK4 during dormancy exit may indicate another pleiotropic role of this transcription factor, but it may also reflect the homology between dormant and asexually reproducing structures.

We found that a retinoic acid (RA) receptor is upregulated in both dormancy and during germination in both species. Additionally, the enzymes retinal dehydrogenase and retinol dehydrogenase show upregulation during germination of *P. zorritensis* and *C. lepadiformis* respectively (Supplementary Figure S2). Together these results are suggestive of a role for RA signaling during germination. RA signaling pathway is implicated in budding in *Polyandrocarpa misakiensis*[85] and whole body regeneration in *Botrylloides leachii*[86]. In our study, we only examined the expression at a single time point during germination, and it is possible that sequence data from more

time points during this process would allow for better resolution of the gene expression dynamics. However, even with this single snapshot, finding shared upregulated genes in germination across distantly related clonal tunicates suggests that these species may employ similar mechanisms in their asexual budding processes. As these species have evolved budding independently from each other, the use of RA signaling in bud formation, if it indeed has a role, would likely represent convergent co-option from its role in embryonic development. Interestingly, up-regulation of RA signaling during dormancy suggests that *P. zorritensis* and *C. lepadiformis* dormant stages functionally represent "arrested buds" at early stages of the budding process.

Conclusions. While the origin of a novel dormant life stage appears to have evolved independently multiple times among asexually replicating tunicates, we have documented a number of ecological, morphological, and cellular convergences across two separate origins of dormancy. In both species, the animal produces a modified stolon filled with nutritive cells and potentially multi/pluripotent cells, which can withstand stressful environments that the adult zooids cannot survive, and is linked to sensing mechanisms to adjust metabolism and time the initiation of budding to when conditions improve. In these cases, dormancy utilizes some of the same cellular and morphological aspects of the budding process that itself evolved independently in each clade, such as the use of the stolon tissues and cells. Our results point to the ways that species reuse existing genes and pathways for the origins of budding and dormancy in tunicates. In particular, our results suggest: (1) conserved eco-physiological sensing mechanisms (e.g., HIF-α signaling) are repeatedly co-opted for the origins of dormancy, as has been found in numerous animals[3], and (2) conserved developmental/regenerative mechanisms (e.g., RA signaling and NK4) are repeatedly co-opted for the origins of budding/germination.

Material and methods

Sample collection and animal husbandry. Colonies of *Polyandrocarpa zorritensis* and *Clavelina lepadiformis* were collected in the harbor of La Spezia, Italy (Assonautica Benedetti, 44°06′10.7″N 9°49′34.5″E). Colonies and spherules of *P. zorritensis* were maintained in the laboratory as reported in Scelzo et al.[38]. Colonies, zooids, and germinating spherules were kept at 24 °C. Spherules were kept at 10 °C. Colonies of *C. lepadiformis* were maintained at 18 °C in a closed sea water system and fed with a mixture of living algae (*Tisochrysis lutea* and *Chaetoceros*) and concentrated algae (Isochrysis 100 and Shellfish Diet 1800, Reed Mariculture Inc, Campbell, CA, USA). *C. lepadiformis* zooids were attached to glass microscope slides with sewing thread and allowed to adhere by stolonal growth at 18 °C for one week. The thread was then removed and the animal was allowed to continue growing until use in experiments. Slides were cleaned twice weekly under a dissecting microscope to remove biofilm and epibiont growth. Microphotographs of animal morphological stages were taken on a Leica M165FC stereoscope.

In order to determine spherule sizes over the course of a year, *P. zorritensis* were collected on three different docks of the marina "Porto Mirabello" during fall (October 2018), winter (January 2019), and spring (May 2019); and spherule diameters were measured. With the aim of following spherule size in a single colony over time (n = 15 per rope per timepoint; n = 45 per timepoint), we repeatedly collected spherules from the same rope at each time point (at marina slips C2, G7, and E15). Diameters (along the longest axis) were calculated from microphotographs using ImageJ. Average spherule diameters were compared using a repeated measures ANOVA conducted in R.

Light and transmission electron microscopy (TEM). In order to visualize the cellular and tissue-level morphology during dormancy and germination, we conducted histology and TEM. Inclusion of dormant and germinating *P. zorritensis* specimens for paraffin sectioning and hematoxylin/eosin staining were performed as described in Alié et al.[82]. Samples of dormant *P. zorritensis* and *C. lepadiformis* for semi-thin and ultra-thin sectioning were fixed, embedded and treated as reported in Scelzo et al.[38].

Effects of environment on dormancy of *P. zorritensis* and *C. lepadiformis*. Adult zooids and dormant stage animals were maintained in aquarium tanks filled with ~ 700 mL sea water with constant aeration in incubators at 24 °C for *P. zorritensis* and 18 °C for *C. lepadiformis* (all at 39 ppt). From this material, we chose specimens to test resistance to temperature and salinity, as described below.

To test the temperature resistance range of zooids and dormancy stages in both species, the specimens were transferred to 50 mL Falcon tubes (Corning, Glendale, Arizona) in filtered sea water and exposed to different temperatures in incubators (− 20 °C, 4 °C, 18 °C, 28 °C, 32 °C, 37 °C) or on ice (for the 0 °C condition) for 24 h (n = 2 for each treatment and each stage). Then, the *P. zorritensis* and *C. lepadiformis* specimens were gradually transferred respectively to 24 °C and 18 °C. For the following 2 weeks, their survival or budding was observed every few days and they were cleaned and fed as in the non-treated specimens.

To test the salinity resistance range of zooids and dormancy stages in both species, animals were exposed to 10 ppt, 15 ppt, 30 ppt, 39 ppt, and 45 ppt salinity water (n = 2 for each treatment and each stage). The low salinity water conditions (10, 15, and 30 ppt) were prepared by adding deionized water to seawater. The high salinity water was prepared by adding artificial sea water to filtered seawater (Red Sea Salt, Red Sea). For each condition, the specimens were transferred to a 50 mL Falcon tube (Corning, Glendale, Arizona) and incubated at 24 °C (*P. zorritensis*) or 18 °C (*C. lepadiformis*) for 24 h. Then, they were gradually transferred to filtered sea water at 39 ppt and observed every few days for the following two weeks.

Differential gene expression analysis. Five life stages were chosen for RNA sequencing of each species: zooid, stolon, prebud (budding nest/chamber), dormant stage, and germination. For each stage, RNA was extracted from three replicate samples. Tissue from three or more specimens (e.g., stolon fragments) was pooled

to obtain enough RNA for each replicate. For the dormant stage *P. zorritensis*, spherules were collected from the field in the spring (the time of the year in which only dormant stages were present) and the tissue was immediately flash-frozen. Additional material from the same rope was transported back to the lab, and germinated to generate new zooids, stolons, and buds, from which we extracted RNA for those stages. For *C. lepadiformis*, we extracted all the material from the same colony in the lab. The "germination" samples were germinated for 48 h, with 3 replicates at 18 °C and 24 °C each. The replicates were combined during analysis because they were not found to be significantly different.

RNA was extracted with the NucleoSpin RNA extraction kit (Machery-Nagel) and sample quality and quantity were verified with the B2100 BioAnalyzer Instrument and Bioanalyzer RNA 6000 Nano assay (Agilent Technologies, Inc., Santa Clara, CA, USA). Frozen RNA was sent for cDNA library preparation (using NEB Next® Ultra RNA Library Prep Kit for Illumina) and Illumina paired-end 150 bp sequencing at Novogene Bioinformatics Technology Co. Ltd (Tianjing, China). Sequencing was done on a Novaseq 6000 PE150 Illumina sequencing platform. Samples were split between two sequencing lanes with at least one of each replicate per stage in each lane to reduce lane-effects.

Raw sequencing reads (541,854,284 for *P. zorritensis* and 521,595,519 for *C. lepadiformis*) were cleaned and trimmed. First, the program Rcorrector was used to correct random sequencing errors and to eliminate read pairs where reads were flagged as 'uncorrectable'[87]. Next, Trim Galore![88] was used to remove low-quality reads from the dataset (with a quality Phred score cutoff of 5, a minimum read length threshold of 36 bp, a stringency parameter of 1 for adapter sequence overlap, and a maximum allowed error rate of 0.1) and to trim Illumina adapters sequences from raw sequencing reads (https://github.com/FelixKrueger/TrimGalore[89]). Ribosomal RNA was removed by eliminating reads that mapped to the SILVA large and small subunit databases (SILVA_132_LSUParc_tax_silva.fasta and SILVA_138_SSURef_NR99_tax_silva.fasta) using Bowtie2[90]. Finally, we used the software FastQC to identify overrepresented sequences from the read set, which we removed[91]. After the preprocessing steps, 496,811,038 reads remained for *P. zorritensis* and 506,081,729 reads remained for *C. lepadiformis*.

Transcriptomes were assembled using the software Trinity with in silico read normalization[92]. For each species, read data after the above preprocessing steps were pooled across tissue types to create a single reference assembly per species. The reference assemblies (809,462 and 492,887 contigs for *P. zorritensis* and *C. lepadiformis*, respectively) were taxon-filtered to remove contaminant transcripts. First, two BLAST searches were conducted to identify possible contaminants: a Diamond Blastx against the uniprot ref database and a blastn search against the NCBI's nr database (both with E-value set to 1e−25). The program Blobtools[93] was used to assign a taxon to each transcript using the blast results (using option "bestsumorder") and then to remove transcripts that were assigned to anything other than chordate, no-hit, or undefined. Proportion of contaminants was 12.5% for *P. zorritensis* and 18.3% for *C. lepadiformis* Next, the program Transdecoder (https://github.com/TransDecoder/TransDecoder) was used to select only the single best open reading frame per transcript, and only keep those with a minimum length of 90. The program cd-hit[94] was used to collapse similar transcripts (parameters: -M 0 -T 20). Low-expression transcripts were removed using Kallisto to estimate abundance and the trinity script "filter_low_expr_transcripts.pl" to remove transcripts with expression level lower than 5 TPM. Final assemblies were 27,938 transcripts for *P. zorritensis* and 18,610 transcripts for *C. lepadiformis*. Assemblies were assessed by looking at basic summary metrics and by quantifying completeness using the program BUSCO (v3) by searching for a curated set of single copy orthologs present in all metazoans (metazoa odb9 database)[95]. BUSCO scores of final reference assemblies were: 68.0% for *P. zorritensis* and 70.7% for *C. lepadiformis,* suggesting that assemblies were relatively complete.

Genes were annotated first by DIAMOND blastx[96] to human refseq database (e-value 1e−25), then those without human ortholog matches, further DIAMOND blastx searches were conducted against the UniProt reference proteome database (e-value 1e−25) to identify lineage-specific transcripts[97]. For *P. zorritensis*, 7,611 transcripts were human-annotated and 1,518 were annotated with non-human matches. For *C. lepadiformis*, 8,037 transcripts were human-annotated and 2,387 were annotated with non-human matches.

The program Kallisto (v. 0.46.0) was used to quantify abundances of transcripts and align preprocessed reads onto the assembled contigs[98]. This was done using scripts bundled with the Trinity package[92]. Mapping rates were 54.2–60.8% for *P. zorritensis* and 60.5–70.9% for *C. lepadiformis*. The Trinity analysis program 'PtR' was used to compare biological replicates across samples, by constructing a correlation matrix for each sample, and principal components analysis (PCA) plots, labeled by stage and replicate.

Differential transcript expression was assessed using the program voom[99] implemented within the Trinity package. All pairwise comparisons of sample type within species were tested. Transcripts were considered differentially expressed if they showed any difference in expression between sample types (C = 0) with a false discovery rate (FDR) *p* value of < 0.001. Heatmaps of the differentially expressed transcripts were generated to cluster the transcripts according to their patterns of differential expression across the samples. Subclusters with genes of similar expression patterns were then calculated by cutting the heatmap by 30% percent tree height for *C. lepadiformis* and 50% tree height for *P. zorritensis*.

In order to identify genes that are consistently upregulated in each tissue/sample-type, we computed tissue-specific expression using perl scripts packaged with Trinity. We selected the "DE_pairwise_summary.txt. class_down_priority" files, which maximizes genes placed into the up-regulated category. Orthologous genes between the two species were identified using a reciprocal best blast hit strategy and the program Blast-Besties (https://github.com/Adamtaranto/blast-besties) using a e-value cutoff of 0.001, a length cutoff of 40 basepairs, and a bitscore cutoff of 100. This generated 6,137 orthologs. Of these orthologs, 4,345 were annotated with human reference data, and 826 did not have human matches but did have close matches in the uniprot proteome database, including many tunicate genes. From the orthologous subset between the two species, we determined the overlapping transcripts upregulated during dormancy and during germination in both species. The data was organized in R and Venn diagrams were produced using the package VennDiagram (v 1.6.0)[100]. The shared

annotated gene lists were used to determine the top over-represented KEGG pathways[101–103]. All annotated transcripts were used as background for the over-representation analysis calculations, which were done with the program DAVID[104,105].

Phylogenetic analysis to confirm gene orthology. Alignments were constructed by performing blastx using *P. zorritensis* or *C. lepadiformis* contigs as queries against *Homo sapiens, Mus musculus, Danio rerio,* Echinodermata, Tunicata and *Drosophila melanogaster* non-redundant protein database (using NCBI blast tool). Aligned sequences were retrieved using vertebrate genes names as an indication to cover putative ingroup and outgroups relative to the ascidians genes. Then alignments were performed using Mafft, trimmed and cleaned manually using BioEdit and analyzed using PhyML under the GTR + G + I model. Trees were visually rooted using treeview. The corresponding ascidian gene orthology was assigned by defining the smallest clade including the target *P. zorritensis* and *C. lepadiformis* contigs together with vertebrate sequences. All the alignments, the resulting phylogenies and the sequence accession numbers are provided in Supplementary Figure S3.

Data availability
The transcriptomic datasets generated in this study are deposited in the Gene Expression Omnibus repository, accession number GSE198056 (https://www.ncbi.nlm.nih.gov/geo/query/acc.cgi?acc=GSE198056).

References
1. Hand, S.C. Metabolic dormancy in aquatic invertebrates. In *Advances in Comparative and Environmental Physiology*, Vol. 8 (ed. Gilles, R.) 1–50. https://doi.org/10.1007/978-3-642-75900-0_1 (1991).
2. Cáceres, C. E. Dormancy in Invertebrates. *Invertebr. Biol.* **116**(4), 371–383. https://doi.org/10.2307/3226870 (1997).
3. Wilsterman, K., Ballinger, M. A. & Williams, C. M. A unifying, eco-physiological framework for animal dormancy. *Funct. Ecol.* **35**, 11–31. https://doi.org/10.1111/1365-2435.13718 (2021).
4. Bertolani, R., Guidetti, R., Altiero, T., Nelson, D. R. & Rebecchi, L. Dormancy in Freshwater Tardigrades. In *Dormancy in Aquatic Organisms. Theory, Human Use and Modeling. Monographiae Biologicae* Vol. 92 (eds Alekseev, V. & Pinel-Alloul, B.) (Springer, Cham, 2019). https://doi.org/10.1007/978-3-030-21213-1_3.
5. Guidetti, R., Altiero, T. & Rebecchi, L. On dormancy strategies in tardigrades. *J. Insect Physiol.* **57**(5), 567–576. https://doi.org/10.1016/j.jinsphys.2011.03.003 (2011).
6. Hahn, D. A. & Denlinger, D. L. Energetics of insect diapause. *Annu. Rev. Entomol.* **56**, 103–121. https://doi.org/10.1146/annurev-ento-112408-085436 (2011).
7. Ragland, G. J. & Keep, E. Comparative transcriptomics support evolutionary convergence of diapause responses across Insecta. *Physiol. Entomol.* **42**(3), 246–256. https://doi.org/10.1111/phen.12193 (2017).
8. Wang, Y., Ezemaduka, A. N., Tang, Y. & Chang, Z. Understanding the mechanism of the dormant dauer formation of *C. elegans*: From genetics to biochemistry. *IUBMB Life* **61**(6), 607–12. https://doi.org/10.1002/iub.211 (2009).
9. Dias, I. B., Bouma, H. R. & Henning, R. H. Unraveling the big sleep: Molecular aspects of stem cell dormancy and hibernation. *Front. Physiol.* **12**, 624950. https://doi.org/10.3389/fphys.2021.624950 (2021).
10. Storey, K. B. & Storey, J. M. Metabolic regulation and gene expression during aestivation. *Prog. Mol. Subcell. Biol.* **49**, 25–45. https://doi.org/10.1007/978-3-642-02421-4_2 (2010).
11. Hand, S. C., Denlinger, D. L., Podrabsky, J. E. & Roy, R. Mechanisms of animal diapause: Recent developments from nematodes, crustaceans, insects, and fish. *Am. J. Physiol. Regul. Integr. Comp. Physiol.* **310**(11), R1193–R1211. https://doi.org/10.1152/ajpregu.00250.2015 (2016).
12. Ikeda, H., Ohtsu, K. & Uye, S. I. Fine structure, histochemistry, and morphogenesis during excystment of the podocysts of the giant jellyfish *Nemopilema nomurai* (Scyphozoa, Rhizostomeae). *Biol. Bull.* **221**(3), 248–260 (2011).
13. Bushnell, J. H. & Rao, K. S. Dormant or quiescent stages and structures among the Ectoprocta: Physical and chemical factors affecting viability and germination of statoblasts. *Trans. Am. Microsc. Soc.* **93**, 524–543. https://doi.org/10.2307/3225156 (1974).
14. Hyman, L. H. *The Invertebrates: Acanthocephala, Aschelminthes and Entoprocta* Vol. III (McGraw-Hill, 1951).
15. Mukai, H. & Toshiki, M. Studies on the regeneration of an entoproct, Barentsia discreta. *J. Exp. Zool.* **205**(2), 261–276. https://doi.org/10.1002/jez.1402050210 (1978).
16. Nakauchi, M. Asexual development of ascidians: Its biological significance, diversity, and morphogenesis. *Am. Zool.* **22**(4), 753–763. https://doi.org/10.1093/icb/22.4.753 (1982).
17. Hyams, Y., Paz, G., Rabinowitz, C. & Rinkevich, B. Insights into the unique torpor of *Botrylloides leachi*, a colonial urochordate. *Dev. Biol.* **428**(1), 101–117. https://doi.org/10.1016/j.ydbio.2017.05.020 (2017).
18. Brown, C. J. D. A limnological study of certain fresh-water Polyzoa with special reference to their statoblasts. *Trans. Am. Microsc. Soc.* **52**, 271–313 (1933).
19. Mukai, H. Development of freshwater bryozoans (Phylactolaemata). In *Developmental Biology of Freshwater Invertebrates* (eds Harrison, R. W. & Cowden, R. R.) 535–576 (Alan R. Liss Inc., 1982).
20. Wood, T. S. Phyla ectoprocta and entoprocta (Bryozoans). In *Freshwater Invertebrates* (eds Thorp, J. H. & Covich, A. P.) 327–345 (Academic Press, 2015). https://doi.org/10.1016/B978-0-12-385026-3.00016-4.
21. Simpson, T. L. *The Cell Biology of Sponges* (Springer, New York, 1984). https://doi.org/10.1007/978-1-4612-5214-6.
22. Alié, A., Hiebert, L. S., Scelzo, M. & Tiozzo, S. The eventful history of nonembryonic development in tunicates. *J. Exp. Zool. Part B Mol. Dev. Evol.* **33**(3), 181–217. https://doi.org/10.1002/jez.b.22940 (2020).
23. Brown, F. D. & Swalla, B. J. Evolution and development of budding by stem cells: Ascidian coloniality as a case study. *Dev. Biol.* **369**2, 151–162 (2012).
24. Kawamura, K. & Fujiwara, S. Cellular and molecular characterization of transdifferentiation in the process of morphallaxis of budding tunicates. *Semin. Cell Biol.* **6**, 117–126 (1995).
25. Kassmer, S. H., Langenbacher, A. D. & De Tomaso, A. W. Integrin-alpha-6+ candidate stem cells are responsible for whole body regeneration in the invertebrate chordate *Botrylloides diegensis*. *Nat. Commun.* **11**(1), 4435–4511. https://doi.org/10.1038/s41467-020-18288-w (2020).
26. Freeman, G. The role of blood cells in the process of asexual reproduction in the tunicate *Perophora viridis*. *J. Exp. Zool.* **156**, 157–183 (1964).
27. Kürn, U., Rendulic, S., Tiozzo, S. & Lauzon, R. J. Asexual propagation and regeneration in colonial ascidians. *Biol. Bull.* **221**(1), 43–61. https://doi.org/10.1086/BBLv221n1p43 (2011).

28. Sköld, H. N., Obst, M., Sköld, M. & Åkesson, B. Stem cells in asexual reproduction of marine invertebrates. In *Stem Cells in Marine Organisms* (eds Rinkevich, B. & Matranga, V.) 105–137 (Springer, Dordrecht, 2009).

29. Tiozzo, S., Brown, F. D. & De Tomaso, A. W. Regeneration and stem cells in ascidians. In *Stem Cells* (ed. Bosch, T. C. G.) (Springer, Dordrecht, 2008). https://doi.org/10.1007/978-1-4020-8274-0_6.

30. Mukai, H., Koyama, H. & Watanabe, H. Studies on the reproduction of three species of Perophora (Ascidiacea). *Biol. Bull.* **164**(2), 251–266 (1983).

31. Huxley, J. Memoirs: studies in dedifferentiation: II. Dedifferentiation and resorption in Perophora. *Q. J. Microsc. Sci.* **s2-65**(260), 643–697 (1921).

32. Huxley, J. Studies in dedifferentiation. VI. Reduction phenomena in Clavelina lepadiformis. *Pubb. Staz. Zool. Napoli.* **7**, 1–34 (1926).

33. Turon, X. Periods of nonfeeding in Polysyncraton-lacazei (Ascidiacea, Didemnidae)—A process. *Mar. Biol.* **112**, 647–655 (1992).

34. Delsuc, F. *et al.* A phylogenomic framework and timescale for comparative studies of tunicates. *BMC Biol.* **16**, 39 (2018).

35. Giard, M. A. & Caullery, M. On the hibernation of *Clavelina lepadiformis*, Müller. *Ann. Mag. Nat. Hist.* **18**(108), 485–486. https://doi.org/10.1080/00222939608680499 (1896).

36. Orton, J. H. The production of living Clavellina Zooids in winter by experiment. *Nature* **107**, 75. https://doi.org/10.1038/107075a0 (1921).

37. Della, Valle P. Studii sui rapporti fra differenziazione e rigenerazione. 4. *Bollettino Della Società Dei Naturalisti in Napoli* **7**, 1–37 (1915).

38. Scelzo, M. *et al.* Novel budding mode in *Polyandrocarpa zorritensis*: a model for comparative studies on asexual development and whole body regeneration. *EvoDevo* https://doi.org/10.1186/s13227-019-0121-x (2019).

39. Berrill, N. J. Regeneration and budding in tunicates. *Biol. Rev.* **26**, 456–475. https://doi.org/10.1111/j.1469-185X.1951.tb01207.x/full (1951).

40. Kilpatrick, K. A., Podestá, G. P. & Evans, R. Overview of the NOAA/NASA advanced very high resolution radiometer Pathfinder algorithm for sea surface temperature and associated matchup database. *J. Geophys. Res.* **106**(C5), 9179–9197. https://doi.org/10.1029/1999JC000065 (2001).

41. Berrill, N. J. & Cohen, A. Regeneration in *Clavelina lepadiformis*. *J. Exp. Biol.* **13**(3), 352–362. https://doi.org/10.1242/jeb.13.3.352 (1936).

42. Jiménez-Merino, J. *et al.* Putative stem cells in the hemolymph and in the intestinal submucosa of the solitary ascidian *Styela plicata*. *EvoDevo* https://doi.org/10.1186/s13227-019-0144-3 (2019).

43. Du, Q., Luu, P.-L., Stirzaker, C. & Clark, S. J. Methyl-CpG-binding domain proteins: Readers of the epigenome. *Epigenomics UK* **7**, 1051–1073 (2015).

44. Rea, S. & Akhtar, A. MSL proteins and the regulation of gene expression. In *DNA Methylation: Development, Genetic Disease and Cancer: Current Topics in Microbiology and Immunology* Vol. 310 (eds Doerfler, W. & Böhm, P.) (Springer, 2006). https://doi.org/10.1007/3-540-31181-5_7.

45. Orton, J. H. Preliminary account of a contribution to an evaluation of the sea. *J. Mar. Biol. Assoc. UK* **10**(2), 312–326. https://doi.org/10.1017/S0025315400007815 (1914).

46. Mukai, H. Histological and histochemical studies of two compound ascidians, *Clavelina lepadiformis* and *Diazona violacea*, with special reference to the trophocytes, ovary and pyloric gland. *Sci. Rep. Fac. Educ. Gunma Univ.* **26**, 37–77 (1977).

47. de Caralt, S., López-Legentil, S., Tarjuelo, I., Uriz, M. J. & Turon, X. Contrasting biological traits of *Clavelina lepadiformis* (Ascidiacea) populations from inside and outside harbours in the western Mediterranean. *Mar. Ecol. Prog. Ser.* **244**, 125–137 (2002).

48. Turon, X. A new mode of colony multiplication by modified budding in the ascidian *Clavelina gemmae* n. sp. (Clavelinidae). *Invertebr. Biol.* **124**(3), 273–283. https://doi.org/10.1111/j.1744-7410.2005.00025.x (2005).

49. Pyo, J. & Shin, S. A new record of invasive alien colonial tunicate *Clavelina lepadiformis* (Ascidiacea: Aplousobranchia: Clavelinidae) in Korea. *Anim. Syst. Evol. Divers.* **27**, 197–200 (2011).

50. Reinhardt, J. *et al.* First record of the non-native light bulb tunicate *Clavelina lepadiformis* (Müller, 1776) in the northwest Atlantic. *Aquat. Invasions* **5**(2), 185–190. https://doi.org/10.3391/ai.2010.5.2.09 (2010).

51. Turon, X., Tarjuelo, I., Duran, S. & Pascual, M. Characterising invasion processes with genetic data: An Atlantic clade of *Clavelina lepadiformis* (Ascidiacea) introduced into Mediterranean harbours. *Hydrobiologia* **503**(1–3), 29–35. https://doi.org/10.1023/b:hydr.0000008481.10705.c2 (2003).

52. Van Name, W. G. The North and South American ascidians. *Bull. Am. Mus. Nat. Hist.* **84**, 1–476 (1945).

53. Carman, M. *et al.* Ascidians at the Pacific and Atlantic entrances to the Panama Canal. *Aquat. Invasions* **6**(4), 371–380. https://doi.org/10.3391/ai.2011.6.4.02 (2011).

54. Holman, L. E. *et al.* Managing human-mediated range shifts: Understanding spatial, temporal and genetic variation in marine non-native species. *Philos. Trans. R. Soc. B* **377**, 20210025 (2022).

55. Lambert, C. C. & Lambert, G. Persistence and differential distribution of nonindigenous ascidians in harbors of the Southern California Bight. *Marine Ecology Progress Series* **259**, 145–161. https://doi.org/10.3354/meps259145 (2003).

56. Brunetti, R. Polyandrocarpa zorritensis (Van Name, 1931). A colonial ascidian new to the Mediterranean record. *Vie et Milieu* **28–29**, 647–652 (1978).

57. Brunetti, R. & Mastrototaro, F. The non-indigenous stolidobranch ascidian *Polyandrocarpa zorritensis* in the Mediterranean: Description, larval morphology and pattern of vascular budding. *Zootaxa* **528**, 1–8 (2004).

58. Mastrototaro, F., D'Onghia, G. & Tursi, A. Spatial and seasonal distribution of ascidians in a semi-enclosed basin of the Mediterranean Sea. *J. Mar. Biol. Assoc. UK* **88**, 1053–1061 (2008).

59. Stabili, L., Licciano, M., Longo, C., Lezzi, M. & Giangrande, A. The Mediterranean non- indigenous ascidian *Polyandrocarpa zorritensis*: Microbiological accumulation capability and environmental implications. *Mar. Pollut. Bull.* **101**, 146–152 (2015).

60. Turon, X. & Becerro, M. A. Growth and survival of several ascidian species from the northwestern Mediterranean. *Mar. Ecol. Prog. Ser.* **82**, 235–247 (1992).

61. Sumida, P. Y. G. *et al.* Pressure tolerance of tadpole larvae of the Atlantic ascidian *Polyandrocarpa zorritensis*: Potential for deep-sea invasion. *Braz. J. Oceanogr.* **63**, 515–520 (2015).

62. Vázquez, E. & Young, C. M. Responses of compound ascidian larvae to haloclines. *Mar. Ecol. Prog. Ser.* **133**, 179–190 (1996).

63. Vázquez, E. & Young, C. M. Ontogenetic changes in phototaxis during larval life of the Ascidian *Polyandrocarpa zorritensis* (Van Name, 1931). *J. Exp. Mar. Biol. Ecol.* **231**, 267–277 (1998).

64. Brien, P. & Brien-Gavage, E. Contribution à l'étude de la Blastogénèse des Tuniciers: III. Bourgeonnement de *Clavelina Lepadiformis* Müller. *Recueil de L'Institut Zoologique Torley-Rousseau* 1–56 (1927).

65. Fujimoto, H. & Watanabe, H. The characterization of granular amoebocytes and their possible roles in the asexual reproduction of the polystyelid ascidian, *Polyzoa vesiculiphora*. *J. Morphol.* **150**(3), 623–637. https://doi.org/10.1002/jmor.1051500303 (1976).

66. Cima, F., Franchi, N. & Ballarin, L. Origin and functions of tunicate hemocytes. In *The Evolution of the Immune System* (ed. Malagoli, D.) 29–49 (Elsevier, 2016). https://doi.org/10.1016/B978-0-12-801975-7/00002-5.

67. Kerb, H. Biologische Beiträge zur Frage der Überwinterung der Ascidien. *Arch. Mikrosk. Anat.* **72**(1), 386–414 (1908).

68. Driesch, H. Studien über das Regulationsvermögen de Organismus. 6. Die Restitutionen der Clavellina lepadiformis. *Arch. F. Entw.-Mech.* **14**, 247–287 (1902).

69. Schultz, E. Über Reductionen. III. Die Reduction und Regeneration des abgeschnitten Kiemenkorbes von *Clavellina lepadiformis*. *Arch. Entw. Mech. Org.* **24**, 503–523 (1907).

70. Spek, J. Über die Winterknospenentwicklung, Regeneration und Reduktion bei *Clavellina lepadiformis* und die Bedeutung besonderer "omnipotenter" Zellelemente für diese Vorgänge. *Wilhelm Roux'Archiv Entwicklungsmechanik der Org* **111**(119), 172 (1927).

71. Brien, P. Contribution à l'étude de la régéneration naturelle et expérimentale chez les Clavelinidae. *Soc. R. Zool. Belg.* **Ann LXI**, 19–112 (1930).

72. Ries, E. Die Tropfenzellen und ihre Bedeutung für die Tunicabildung bei Clavelina. *Wilhelm Roux Arch. Entwickl. Mech. Org.* **137**(3), 363–371. https://doi.org/10.1007/BF00593066 (1937).

73. Fischer, I. Über das Verhalten des stolonialen Gewebes der Ascidie *Clavelina lepadiformis* in vitro. *Wilhelm Roux Arch. Entwickl. Mech. Org.* **137**(3), 383–403. https://doi.org/10.1007/BF00593068 (1937).

74. Seelinger, O. Eibildung und Knospung von *Clavelina lepadiformis*. *Sitzungsber. d. Kais. Kgl. Acad. d. Wiss* 1–56 (1882).

75. Van Beneden, E. & Julin, C. Recherches sur la morphologie des tuniciers. *Arch. Biol.* **6**, 237–476 (1886).

76. Garstang, W. Memoirs: The morphology of the Tunicata, and its bearings on the phylogeny of the Chordata. *J. Cell Sci.* **1928**(2), 51–187 (1928).

77. Kimura, K. D., Tissenbaum, H. A., Liu, Y. X. & Ruvkun, G. daf-2, an insulin receptor-like gene that regulates longevity and diapause in *Caenorhabditis elegans*. *Science* **277**, 942–946 (1997).

78. Ogawa, A. & Brown, F. Dauer formation and dauer-specific behaviours in *Pristionchus pacificus*. In *Pristionchus pacificus—A nematode model for comparative and evolutionary biology* (ed. Sommer, R. J.) (Brill, 2015). https://doi.org/10.1163/9789004260306_011.

79. Wisdom, R. AP-1: One switch for many signals. *Exp. Cell Res.* **253**(1), 180–185. https://doi.org/10.1006/excr.1999.4685 (1999).

80. Karin, M., Liu, Z. & Zandi, E. AP-1 function and regulation. *Curr. Opin. Cell Biol.* **9**, 240–246 (1997).

81. Srivastava, M. Beyond casual resemblances: rigorous frameworks for comparing regeneration across species. *Annu. Rev. Cell Dev. Biol.* **37**, 1–26 (2021).

82. Alié, A. *et al.* Convergent acquisition of nonembryonic development in styelid ascidians. *Mol. Biol. Evol.* **35**, 1728–1743. https://doi.org/10.1093/molbev/msy068 (2018).

83. Wang, W., Razy-Krajka, F., Siu, E., Ketcham, A. & Christiaen, L. NK4 antagonizes Tbx1/10 to promote cardiac versus pharyngeal muscle fate in the ascidian second heart field. *PLoS Biol.* **11**, 1. https://doi.org/10.1371/journal.pbio.1001725 (2013).

84. Prünster, M. M., Ricci, L., Brown, F. D. & Tiozzo, S. Modular co-option of cardiopharyngeal genes during non-embryonic myogenesis. *EvoDevo* https://doi.org/10.1186/s13227-019-0116-7 (2019).

85. Kawamura, K., Shiohara, M., Kanda, M. & Fujiwara, S. Retinoid X receptor-mediated transdifferentiation cascade in budding tunicates. *Dev. Biol.* **384**, 343–355 (2013).

86. Rinkevich, Y., Paz, G., Rinkevich, B. & Reshef, R. Systemic bud induction and retinoic acid signaling underlie whole body regeneration in the urochordate *Botrylloides leachi*. *PLoS Biol.* **5**, e71. https://doi.org/10.1371/journal.pbio.0050071 (2007).

87. Song, L. & Florea, L. Rcorrector: Efficient and accurate error correction for Illumina RNA-seq reads. *GigaScience.* **4**(1), 48. https://doi.org/10.1186/s13742-015-0089-y (2015).

88. Krueger, F. Trim Galore!: A wrapper tool around Cutadapt and FastQC to consistently apply quality and adapter trimming to FastQ files. http://www.bioinformatics.babraham.ac.uk/projects/trim_galore/ (2015).

89. Martin, M. Cutadapt removes adapter sequences from high-throughput sequencing reads. *EMBnet J.* **17**(1), 10–12. https://doi.org/10.14806/ej.17.1.200 (2011).

90. Langmead, B. & Salzberg, S. L. Fast gapped-read alignment with Bowtie 2. *Nat. Methods* **9**(4), 357–359. https://doi.org/10.1038/nmeth.1923 (2012).

91. Andrews, S. FastQC: A quality control tool for high throughput sequence data. http://www.bioinformatics.babraham.ac.uk/projects/fastqc (2010).

92. Grabherr, M. G. *et al.* Full-length transcriptome assembly from RNA-Seq data without a reference genome. *Nat. Biotechnol.* **29**, 644–652. https://doi.org/10.1038/nbt.1883 (2011).

93. Laetsch, D. R. & Blaxter, M. L. BlobTools: Interrogation of genome assemblies. *F1000Research* **6**, 1287. https://doi.org/10.12688/f1000research.12232.1 (2017).

94. Li, W. & Godzik, A. Cd-hit: A fast program for clustering and comparing large sets of protein or nucleotide sequences. *Bioinformatics* **22**(13), 1658–1659. https://doi.org/10.1093/bioinformatics/btl158 (2006).

95. Seppey, M., Manni, M. & Zdobnov, E. M. BUSCO: Assessing genome assembly and annotation completeness. In *Gene prediction* (ed. Kollmar, M.) 227–245 (Humana, New York, 2019). https://doi.org/10.1007/978-1-4939-9173-0_14.

96. Buchfink, B., Reuter, K. & Drost, H. G. Sensitive protein alignments at tree-of-life scale using DIAMOND. *Nat. Methods* **18**, 366–368. https://doi.org/10.1038/s41592-021-01101-x (2021).

97. The UniProt Consortium. UniProt: The universal protein knowledgebase in 2021. *Nucleic Acids Res.* **49**(D1), D480–D489. https://doi.org/10.1093/nar/gkaa1100 (2021).

98. Bray, N. L., Pimentel, H., Melsted, P. & Pachter, L. Near-optimal probabilistic RNA-seq quantification. *Nat. Biotechnol.* **34**(5), 525–527. https://doi.org/10.1038/nbt.3519 (2016).

99. Law, C. W., Chen, Y., Shi, W. & Smyth, G. K. voom: Precision weights unlock linear model analysis tools for RNA-seq read counts. *Genome Biol.* **15**(2), 1–17. https://doi.org/10.1186/gb-2014-15-2-r29 (2014).

100. Chen, H. & Boutros, P. C. VennDiagram: A package for the generation of highly-customizable Venn and Euler diagrams in R. *BMC Bioinform.* **12**(1), 35. https://doi.org/10.1186/1471-2105-12-35 (2011).

101. Kanehisa, M. Toward understanding the origin and evolution of cellular organisms. *Protein Sci.* **28**, 1947–1951. https://doi.org/10.1002/pro.3715 (2019).

102. Kanehisa, M. & Goto, S. KEGG: Kyoto encyclopedia of genes and genomes. *Nucleic Acids Res.* **28**(1), 27–30. https://doi.org/10.1093/nar/28.1.27 (2000).

103. Kanehisa, M., Furumichi, M., Sato, Y., Ishiguro-Watanabe, M. & Tanabe, M. KEGG: Integrating viruses and cellular organisms. *Nucleic Acids Res* **49**(D1), D545–D551. https://doi.org/10.1093/nar/gkaa970 (2021).

104. Huang, D. W., Sherman, B. T. & Lempicki, R. A. Systematic and integrative analysis of large gene lists using DAVID bioinformatics resources. *Nat. Protoc.* **4**(1), 44–57 (2009).

105. Huang, D. W., Sherman, B. T. & Lempicki, R. A. Bioinformatics enrichment tools: Paths toward the comprehensive functional analysis of large gene lists. *Nucleic Acids Res.* **37**(1), 1–13 (2009).

Acknowledgements

Author contributions

L.H., S.T. and F.D.B. conceived and designed the study; L.H. and M.S. performed the experiments; L.H. assembled the transcriptomes and analyzed the RNAseq dataset; A.A. performed the phylogenetic analyses; L.H., S.T. and F.D.B. wrote and edited the manuscript. All authors read and commented on drafts, and approved the final version.

Competing interests

The authors declare no competing interests.

Additional information

Supplementary Information The online version contains supplementary material available at https://doi.org/10.1038/s41598-022-16656-8.

Correspondence and requests for materials should be addressed to F.D.B. or S.T.

Reprints and permissions information is available at www.nature.com/reprints.

Publisher's note Springer Nature remains neutral with regard to jurisdictional claims in published maps and institutional affiliations.